Morphological Differences of the Articulating Surfaces of Mandibular Condyles in C3H/HeJ and A/J Mice

Neker E. Bernuy, DDS

A thesis submitted to the faculty of the University of North Carolina at Chapel Hill in partial fulfillment of the requirements for the degree of Master of Science in the School of Dentistry (Orthodontics).

Chapel Hill
2013

Approved by:

Dr. Eric T. Everett

Dr. Lucia Cevidanes

Dr. Emile Rossouw

Dr. Sylvia Frazier-Bowers

ABSTRACT

NEKER E. BERNUY: Morphological Differences of the Articulating Surfaces of Mandibular Condyles in C3H/HeJ and A/J Mice
(Under the direction of Dr. Eric T. Everett)

Objectives: Characterize the normal variation of the articulating surfaces of mandibular condyle morphologies during periods of growth within and between two strains of mice (A/J and C3H/HeJ) using 3D micro-CT analysis and determine which parts of the microanatomy of the articulating surfaces of the condyle are less susceptible to morphologic variation during skeletal growth. **Methods:** Cross sectional study utilized micro-CT scans of the condyles of two strains of mice (A/J and C3H/HeJ) at 3-5 wks, 6-8 wks and 9-11 wks of age. Virtual 3D surface models were created, analyzed and computed using shape analysis methods. **Results:** There is inter-strain variation in condyle morphologies among inbred strains and at each age group. For A/J condylar growth the greatest differences in morphologic change occurs between 3-5 weeks and 6-8 weeks of age with little change thereafter. For the C3H/HeJ strain condylar growth and morphology continued to change beyond 6-8 weeks of age. The anterior and the posterior surfaces of the condyles tended to vary greatest in morphology. **Conclusions:** Condyles of A/J inbred of mice reach a morphologic plateau around 6-8 weeks of age whereas C3H/HeJ inbred of mice condyles continue morphologic change and growth after 6-8 weeks. Inbred mice despite being isogenic still present shape differences in anatomical structures such as the condyle.

. **ACKNOWLEGEMENTS**

I would like to thank the following for their significant contributions to this project:

Dr. Eric Everett: For his helpful guidance and contribution to the success of this project.

Dr. Lucia Cevidanes: For her enormous cooperation to the research, invaluable guidance, constructive comments and friendly encouragement during the thesis work.

Dr. Emile Rossouw: For his significant contribution to this work, assistance, and constructive comments for the improvement of the manuscript.

Dr. Frazier-Bowers: For her thoughtful insight, support and direction.

Drs. Tung Nguyen and Beatriz Paniagua: For their insight and expertise provided during the development as well as preparation of this project.

I would like to thank my parents for their love, patience and continued support in this journey in my life that started 10 years ago. I also thank my best friend and partner in everything Angela for her continued support and motivation. Their sacrifices have allowed me to pursue my dreams and ambitions.

TABLE OF CONTENTS

LIST OF TABLES vi

LIST OF FIGURES vii

I. LITERATURE REVIEW 1

THE TEMPOROMANDIBULAR JOINT DISEASE 1

ANIMAL MODEL AND RATIONALE FOR SELECTING STRAINS TO STUDY TMJ MORPHOLOGIES 13

THE USE OF A MOUSE MANDIBLE AS A MODEL TO STUDY DEVELOPMENT AND EVOLUTION OF COMPLEX TRAITS 21

MORPHOMETRICS ANALYSIS 25

IMAGE ANALYSIS PROCEDURES 33

REFERENCES 38

II. MANUSCRIPT 46

INTRODUCTION 46

MATERIALS AND METHODS 49

RESULTS 53

DISCUSSION 57

CONCLUSIONS 62

FIGURES 63

TABLES 73

REFERENCES 75

LIST OF TABLES

Table 1. Origin and insertion of muscles of mastication 4

Table 2. Signs and symptoms observed in patients with TMD 7

Table 3. Maximum difference values between A/J and C3H/HeJ strains at 3-5 weeks, 6-8 weeks and 9-11 weeks of age 73

Table 4. Maximum difference values among A/J strains of mice at 3-5 weeks, 6-8 weeks and 9-11 weeks of age 73

Table 5. Maximum difference values among C3H/HeJ strains of mice at 3-5 weeks, 6-8 weeks and 9-11 weeks of age 74

LIST OF FIGURES

Figure 1. Methodology used for shape analysis of the condyles..... 63

Figure 2. Composite average surface models for each age group, strain and side..... 63

Figure 3. Shape analysis between A/J and C3H/HeJ strains at 3-5 weeks of age..... 64

Figure 4. Shape analysis between A/J and C3H/HeJ strains at 6-8 weeks of age..... 64

Figure 5. Shape analysis between A/J and C3H/HeJ strains at 9-11 weeks of age..... 65

Figure 6. A/J shape analysis at 3-5 weeks and 6-8 weeks of age..... 65

Figure 7. A/J shape analysis at 6-8 weeks and 9-11 weeks of age..... 66

Figure 8. A/J shape analysis at 3-5 weeks and 9-11 weeks of age..... 66

Figure 9. C3H/HeJ shape analysis at 3-5 weeks and 6-8 weeks of age 67

Figure 10. C3H/HeJ shape analysis at 6-8 weeks and 9-11 weeks of age. 67

Figure 11. C3H/HeJ shape analysis at 3-5 weeks and 9-11 weeks of age 68

Figure 12. Individual morphological variability of the A/J strain at 3-5 weeks of age..... 69

Figure 13. Individual morphological variability of the A/J strain at 6-8 weeks of age..... 69

Figure 14. Individual morphological variability of the A/J strain at 9-11 weeks of age..... 70

Figure 15. Individual morphological variability of the C3H/HeJ strain at 3-5 weeks of age 71

Figure 16. Individual morphological variability of the C3H/HeJ strain at 6-8 weeks of age 71

Figure 17. Individual morphological variability of the C3H/HeJ strain at 9-11 weeks of age 72

I. LITERATURE REVIEW

1. THE TEMPOROMANDIBULAR JOINT DISEASE

Temporomandibular joints (TMJs) are bilateral synovial joints that play crucial roles in the process of speech, mastication, and deglutition. TMJs are key structures in the craniomandibular apparatus because they allow movement of the mandible in three planes of space, antero-posterior, vertical, and lateral movements. During growth and development of the craniomandibular complex, TMJs influence upper and lower jaw relationships, occlusion, and the masticatory system. Temporomandibular joint disorder (TMD) is described as functional and structural abnormalities of the muscles, tendons, ligaments, blood vessels, and other tissues associated with the temporomandibular joint [1, 2].

The debilitating effects of TMD include muscle stiffness, locking of the jaw and radiating pain in the face, jaw and neck. It is estimated that 75% of the U.S. population may experience TMD at least once in their lifetime with more prevalence in women than in men. The research indicates that, during any given year, 10% of women and 6% of men have TMD pain, which translates to 20 million adults. [3]

1.1. *Joint Embryology*

Descriptively, there are three stages of TMJ development. The first stage of formation is called the blastematic stage and occurs during weeks 7 and 8 of development in humans. This stage is also defined by the mesenchymal condensation of the condyle

and formation of the articulating disc and capsule. During the first stage, the formation of the TMJ cavity is delayed and is not visible. The second stage is termed the cavitation stage, which occurs around weeks 9 to 11 of development. During this stage, the development of the inferior region of the joint cavity occurs on the squamous part of the temporal bone by intramembranous ossification, and the initiation of condylar chondrogenesis occurs as well. The third stage of development, the maturation stage, begins during week 12. During this stage, no significant changes are observed because the joint cavity is already well defined; hence, we can observe a well demarcated tympanosquamosal fissure fully formed on the squamous portion of the temporal bone. By week 14, Meckel's cartilage has undergone a significant anatomical volume reduction and by week 17, consolidation of the anterior portion of the condyle and the lateral pterygoid muscle has been established. During this final stage, we observe the last anatomical incorporation between the lateral pterygoid muscle, the condyle and the antero-internal two-thirds of the articular disc. [4]

1.2. *Joint Anatomy*

The TMJ consists of many components that work as a unit, these are: the mandibular condyle, the temporomandibular fossa, the articular disc, the joint capsule, the ligaments, the muscles of mastication and the blood and nerve supply. The mandibular condyle is one of two vertical projections upwards along with the coronoid process. The condyles originate in the body of the mandible and are described as a cylindrically shaped and narrowing from the anterior-posterior side. Bernard (2001) provides an approximate measurement of the condyle of 13 mm high by 25 mm wide (mediolaterally) [2, 5].

The second component is located on the squamous region of the temporal bone; this anatomical structure is the temporomandibular fossa. Anteriorly, it is bound by the articular tubercle and posteriorly by the tympanic part of the bone. It is divided into two parts by the petrotympanic fissure.

The third component is the articular disc, also called “the meniscus”, which has a saddle shape and functions to separate the condyle from the temporal bone. The meniscus has a fibrous consistency due to its bands, which vary in thickness [5]. These bands are classified according to thickness with the thin portion at the central intermediate zone; the first thick portion, also called the anterior band, at the posterior articular eminence; and a second thick band, attached to the back of the posterior wall of the mandibular fossa and the squamo-tympanic suture, which was described and named as the posterior bilaminar zone. The location of this band is at the most posterior region of the condylar head [2, 5].

Four areas of fibrocartilage can be observed in the articular region of the mandibular condyle and its articulating disc. The first area, called the articular area, is part of the most superficial layer and is rich in proteoglycan 4 (PRG4) which functions to lubricate the joint. The second area is rich in precursor cells for the flattened and hypertrophic areas; it is called the polymorphic zone. The third area is called the flattened zone, and the fourth and deepest area is the hypertrophic zone. It is in this last area (the hypertrophic zone) that collagen type X (Col X) expression characterizes the chondrocytes. [2, 6, 7] This disc is kept in place by attachments at the articular eminence and the anterior region of the condyle. It also receives attachments from the lateral pterygoid muscle anteriorly, from the glenoid fossa posteriorly, and the neck of the condyle distally; all of which help the articulating disk remain in a secure position. [5].

Another crucial component of the TMJ is the joint capsule. Its role is to enclose the joint with its thin consistency to provide stabilization for the complex movements and functions of this articulation. Three ligaments form part of the joint capsule. The major one is the temporomandibular ligament, and the two minor ligaments are the sphenomandibular and stylomandibular ligaments. The muscles that are part of the TMJ are the masseter, the temporalis, the lateral pterygoid and the medial pterygoid. Their origin and insertion are described in (Table 1). [5]

Table 1. Origin and insertion of muscles of mastication

MUSCLE	ORIGIN	INSERTION
Masseter	**Superficial head:** Anterior two thirds of the lower border of the zygomatic arch **Deep head:** Posterior one third and medial surface of the zygomatic arch	**Superficial head:** Angle of mandible **Deep head:** Ramus of mandible
Temporalis	Temporal fossa	Coronoid process of mandible
Lateral pterygoid	**Superior head:** Greater wing of the sphenoid bone **Inferior head:** Lateral plate of the sphenoid bone	**Both heads:** Pterygoid fovea of the mandible
Medial pterygoid	Pterygoid fossa of the sphenoid bone	Angle of mandible

1.3. *Etiology of TMD*

Temporomandibular Disorders (TMDs) are developmental and acquired pathologies of the hard and soft tissues of the TMJs which affect the size, the form and the functional relationship of the components of the TMJs. TMDs have become common conditions with very high treatment costs. The etiology of TMDs is multifactorial. Excluding trauma or inflammatory diseases (i.e. rheumatoid arthritis), there is

considerable controversy among investigators regarding other possible causes of TMD. Many theories have evolved, which seem to be designed to justify a particular therapy rather than address the actual cause of the disorder [8].

Trauma to the temporomandibular joint can trigger development of symptoms related to TMD, but may not necessarily initiate the disorder. Trauma due to automobile accidents (e.g. whiplash) is one of the most common causes of TMD. The disorder may also arise from a blow to the face resulting in damage or fracture of the condyles which precipitate an alteration in the function of the TMJ. This alteration can be due to the stretching of the ligaments or the formation of scar tissue due to internal bleeding [9]

Diseases such as rheumatoid arthritis, gout, neoplasia and osteoarthritis also play major roles in the etiology of TMDs. In these disease processes, the inflammatory condition disturbs the equilibrium between the destruction and the repair of joint tissue, thereby compromising its integrity. Osteoarthritis has been a topic of several major research studies due to its progressive nature, in which degeneration of the joint occurs by bony changes and destruction of the disc, ultimately resulting in muscle pain and compromised function of the TMJ [10].

Congenital and genetic factors can also influence the onset of TMD, and research now suggests a relationship between serotonin receptors and TMD. A study conducted by Mutlu (2004) considered the association between T102C polymorphism of the 5-hydroxytryptamine (serotonin) receptor 2A, G protein-coupled (HTR2A) receptors and temporomandibular disease. Participants in this study consisted of 63 patients with clear symptoms and signs of TMD and 54 healthy patients. Using polymerase chain reaction (PCR), they analyzed the T102C polymorphism of the *HTR2A* receptor gene. Their

results showed that in the healthy patients, the T/T genotype was over-represented, while in the patients with TMD, the C/C genotype was over-represented. They concluded that TMD development may be related to the T102C polymorphism. Despite these findings the overall amount of research done in this field is low, and the results are inconclusive [11].

An additional cause of TMD may be alterations in the stomatognathic system that can occur as a result of changes in posture and parafunctional habits (e.g., bruxism, teeth clenching, and lip biting). These factors may create a predisposition for the development of TMD [12]. Even though parafunctional habits have been thought to cause TMJ, microtrauma and muscle hyperactivity than can lead to TMD. These habits are also present in asymptomatic patients, creating a weak relationship between parafunctional habits and TMD. The prevalence of bruxism reported by Seligman (1988) showed that a higher number of patients experienced bruxism when they were evaluated clinically (48-58%) than when they were assessed by questionnaire (8-21%)[13]. Buescher (2007) suggested that psychosocial factors such as anxiety, stress, depression and other emotional disturbances exacerbate temporomandibular disease, especially in patients who experience chronic pain. Regardless of the differences of opinions about the influence of habits and head posture that may lead to the development of TMD, anything that could aggravate a pre-existing condition should be avoided. [12, 13]

The characteristic symptoms of TMD are muscle pain or discomfort, limited mandibular motion, disc displacement, disc dislocation, temporomandibular joint sounds and arthralgia [12]. Patients also report associated symptoms, such as headache, neck pain, back pain, toothache, tinnitus and dizziness [8]. Finally, TMD may culminate in

facial pain that leads to related disabilities affecting the jaw, tooth position, and occlusion. Occlusal changes associated with these pathological conditions include a progressive anterior open bite and limitation or deviation of jaw movements (Table 2) [1, 14-16].

Table 2. Signs and symptoms observed in patients with TMD

DENTAL DESTRUCTION	DYSFUNCTIONAL SYMPTOMS	PAINFUL SYMPTOMS
• Traumatic occlusion • Clenching • Grinding • Bruxism • Excessive wear • Abrasion of the dentition	• Limited jaw movement • Deviated jaw movement • Slow or irregular jaw movement • Limited range of motion • Joint sounds such as clicking or crepitus • Locked or dislocated jaw	• Headaches • Facial pain • Pain in the jaw joints • Ear pain • Ear pressure • Neck, shoulder and chest pain

1.4. *Epidemiology of TMD*

The reported prevalence of this disorder varies widely depending on the methodologies and definitions used to diagnose it. Proffit et al (2000) provided an estimation of the incidence of new cases of TMD based on recorded signs and symptoms, indicating that 5-35% of the population would be affected, which is a much lower number than the 50% of the population experiencing a degree of malocclusion above the normal limits (moderate malocclusion). The American Academy of Orofacial Pain estimates that 75% of the U.S. population may experience TMD at least once in their lifetime. The condition has been is more prevalent in women than in men, with the research indicating that, during any given year, 10% of women and 6% of men have TMD pain, which translates to 20 million adults [3]. According to Wiese (2008), about

49% of patients with TMD pain presented with some kind of radiographic osseous change. [17]

It is estimated that for the 5.3 million U.S. residents who seek treatment for TMD, the cost will be approximately $2.3 billion. TMD was reported to have a significant impact on productivity; 28% of TMD patients were affected to such an extent that they had a limited ability to continue at their current jobs. With this in mind, the projected costs of TMD, based on estimates of the indirect and direct costs outlined by the above researchers, are estimated to be over $4 billion a year [18, 19].

TMD is a problem for other developed nations as well. A study done on Swedish adolescents by Nilsson (2005) demonstrated that 4.2% of 28,899 participating youths between 12-19 years of age reported TMD pain. Moreover, the prevalence of the disorder increased with age and females (6.0%) were more likely to be affected than males (2.7%) [20]. This contradicts earlier research which found that males and females were affected equally [21]. Recent studies indicate that females have a higher prevalence of TMD than males [22]. The research of LeResche (2003) supports that the perception of pain fluctuates in females in concordance with their menstrual cycles and pain is highest during pre-menstruation and menses. More research is needed to determine why females are more predisposed to TMD than males [23]. A groups affected by TMD, were assessed in a study by Locker (1988). They found that the frequencies of pain in individuals under the age of 45 (8.3%) were slightly higher than in individuals 45 years of age and older (7.2%) [24].

1.5. *Developmental and Environmental Effects on TMJ*

Developmental and environmental stimuli have been shown to affect craniomandibular morphology including hormonal, vascular, biomechanical and dietary factors. Mechanical stress induced by mastication also affects the mandible especially around the masticatory muscles and mandibular condylar cartilage, as well as progressive changes to the pattern of development and growth of the mandible. Bouvier (1981) demonstrated differences between growing monkeys raised on a hard food diet and those raised on a soft diet.

> "Monkeys raised on hard diets showed more cortical bone remodeling, higher density connective tissue, higher subchondral bone, thicker condylar articular cartilage, and greater mandibular depth and cortical bone thickness compared to the temporomandibular joint of soft diet macaques" [25].

Tuominen (1993) demonstrated that the mandible of rabbits change shape with different diets and that functional stress influences the shape of the articular eminence and the intermaxillary relationship [26]. Additionally, another study on rats evaluated the ramus heights of two different diet groups and demonstrated that rats fed with hard diets presented with greater ramus heights than those fed with soft diets. Furthermore, a different study where the condylar dimensions were evaluated in different diet groups showed that rats fed a hard diet presented with greater condyle dimensions and greater spongiosa volumes compared with rats fed a soft diet, because the lateral and inferior periosteal bone growth, along with condylar elongation, were slowed with the soft diet [27].

Difference in mastication load between hard and soft diets have demonstrated that an increased load of force on the temporomandibular joint occurred in the hard diet group compared to animals in the soft diet group [28]. Bouvier (1988) has shown histologically

that the hypertrophic chondrocyte zone of mandibular condylar cartilage experiences a change in thickness in rats fed on a hard diet. There are several rat and rabbit studies that have evaluated the effects of altering TMJ force application by differing loading regimens, tooth extraction, incisor trimming, unilateral bite rise or corticotomy, all of which have been shown to result in gene expression changes and elevated glycosaminoglycan (GAG) levels in condylar cartilage [26, 29, 30]. In contrast, a study by Chen (2009) demonstrated in an altered functional loading mouse model where the incisor teeth are trimmed frequently and animals placed on a soft diet demonstrated morphological changes in the condylar heads and altered expression of *Col2a1*, *Vegfa*, *Col1a1*, *Tnfsf11* and *Sox9* genes compared to the normal masticatory loaded (standard mouse chow hard diet) group after 6-weeks.[31]

1.6. *Genetic Control of TMJ Development*

TMJ components and anatomical structures are well-documented and described by several authors, but information regarding the molecular mechanisms for TMJ morphogenesis is poorly understood. Abnormalities in the development of the mandible in mice, specifically in the TMJ, can be a consequence of the inactivation of certain molecules that regulate outgrowth and morphogenesis of the mandibular arch and its skeletal elements [32]. The findings in these mice provide powerful evidence for the importance of signaling molecules involved in mandibular morphogenesis. There is evidence that in early-stage mouse embryos, regionally restricted expression of homeotic genes, such as members of the *Msx, Dlx, Lhx, Otx, Barx, Gsc, Pax, Hand, Pitx and Prx* families, may be responsible for causing early polarity at the first brachial arch, thus establishing the baseline for the development of mandibular skeletal elements. It is

important to mention that members of the fibroblast growth factor (Fgf), bone-morphogenetic protein (Bmp), endothelin (ET), hedgehog (Hh), platelet-derived growth factor (Pdgf) and epidermal growth factor (Egf) families of signaling molecules induce regional expression of downstream target genes in the ectomesenchyme [32, 33] .

Many gaps in the knowledge exist, particularly a complete understanding of the genetics behind the development of the TMJ as a synovial joint. Several components of the Hh signaling pathway are expressed in the condyle and disk of the developing TMJ. It was demonstrated that mice deficient in the gene *Gli2* displayed abnormal TMJ development to the extent that the growth-plate-like cellular organization is lost, and the TMJ does not form a disk. The formation of the TMJ disk is a two-step process, dependent upon Hh signaling. First, there is basic disk formation, which is then followed by disk maturation and culminates in separation from the condyle and formation of the lower joint cavity [34].

Notably, Purcell (2012) provided evidence that the TMJ condyle and disc develop independently of the mandibular fossa. They showed that sprouty genes (*Spry*) encode intracellular inhibitors of receptor tyrosine kinase (RTK) signaling pathways, including those triggered by fibroblast growth factors (Fgfs). *Fgfr4* and *Spry* genes play an important role in the development of various organs, including the ear, teeth, lenses, mandible, palate, and muscles, but as they pertain to the TMJ, they are highly expressed in the attached muscles (the lateral pterygoid and temporalis, for example). When both genes are inactivated, the muscles grow unchecked, become overgrown, and prevent normal development of the glenoid fossa [35].

It is remarkable that in mutant mice, condyle and disc formation are not affected, suggesting that the glenoid fossa is not necessary for development of these structures. Future studies should explore how sprouty genes and other muscle growth and differentiation signals are related, as well as how these affect fossa formation. [35]

Further molecular understanding of TMJ organogenesis is essential for improving diagnosis and developing new therapeutic approaches for TMJ disorders. Phenotypic analyses of animals in which candidate genes are overexpressed in the developing mandible may provide the needed information about the roles of gene products. The phenotypic characterization at each developmental stage of mice with a known genetic background that are subject to controlled environmental factors has the potential to differentiate between the developmental effects of growth, as well as lead to the development of tools for diagnosing pathological phenotypes in temporomandibular joint disorders [32] .

The morphology of the TMJ is determined by the composite of genetic and environmental factors controlling its development. Studies on fluctuating asymmetry (small random differences in the development of left and right body sides of individuals) have been proposed as a way to control for genetic and environmental factors because both sides of the same individual or animal share the same genome and nearly the same environment. The expression of right and left differences may highlight the role of developmental and functional differences that affect each condyle's morphology [36].

2. ANIMAL MODEL AND RATIONALE FOR SELECTING STRAINS TO STUDY TMJ MORPHOLOGIES

2.1. *Role of Mice in Biomedical Research*

Rodents are recognized as a useful animal model for biomedical research. Through the routine use of recombinant DNA and the ability to isolate cloned copies of genes and compare DNA of different organisms, we have learned that placental mammals, including mice and humans, are much more genetically similar than previously believed. Since mouse and rat embryonic development parallels that of humans, we are able to study their genetic development to provide information about complex traits in humans. Also, their utility as model organisms is enhanced by our ability to modify their genomes (transgenic and gene targeted animals) [37].

Additional advantages that mice provide are low cost, short gestation time (19–21 days, depending on the strain), short generation time (10 weeks from being born to giving birth), females reproduce prolifically in the lab with an average of 5-10 pups per litter, and mice have an accelerated lifespan. These advantages permit studies to be conducted and completed within a few years, rather than the decades it would take to study larger mammals. The value of mice also comes from their sharing many complex diseases with humans, i.e. cancer, aging, arthrosclerosis, and diabetes [38]. It is important to mention that, among mammals, the mouse is second only to humans in the frequency and variety of spontaneous cancers it may develop, which makes it an excellent instrument for research in the cancer field [39].

Mice strains have been shown to exhibit diseases and characteristics similar to those of humans. This similarity permits the investigation of the pathogenesis of disease

and progression in a manner not always possible in humans. The easy manipulation of the mouse's genetic makeup allows the development of new strains with gene knockout, gene overexpression and genetic breeding strategies [40]. Furthermore, we already know that human genetic characteristics are similar to those of mice; with the exclusion of identical twins, the genetic load in human beings differs significantly from one person to another, making studies of genetic variation in humans very difficult. Well-distinguished animal lines, such as murine inbred strains, can be engineered to have phenotypes related to human disease, and are consequently used to study and analyze homogeneous populations [37, 38]. Another advantage of working with inbred strains is the potential for reproducing and advancing experiments involving genetically uniform mice; researchers can be confident that the mice used in experiments today are almost genetically identical to mice of the same strain used years ago. Genetic similarities in mice make it easier for researchers to understand complex traits, diseases, susceptibilities and adaptations which occur in mice and later use that information to make conclusions about humans, who are more genetically diverse. Finally, many strains of laboratory mice exist. In order to conduct effective research, it is important to understand the origin and the history of a particular mouse strain to effectively make relevant findings with controlled variability[37, 39, 40].

2.2. *Origin Of The Mouse*

The origin of the mouse can be traced back to the end of the ice age (10,000 years ago) to areas in modern-day Israel, Lebanon and Syria. These geographical regions formed the Fertile Crescent, an area where tribes of nomadic hunters and gatherers began domestication of animals and developed techniques of cultivating plants [37, 41]. The

development of farming and domestication of animals led to the establishment of permanent villages where people would store dry grains they had harvested in shelters. The storage of food in granaries and cupboards created the perfect environment for mice, and thus began their longstanding relationship with humankind [37]. Mice followed humans as they wandered from their villages in the Middle East in search of new lands to cultivate. They were able to board merchant ships, which carried them off to distant lands throughout the inhabited world. In many parts of the world with harsh natural environments, human habitation provided mice with the shelter necessary for their survival. Today, mice can be found wherever human settlements exist, in both rural and urban areas, extending to the north and south of both hemispheres, and even at altitudes as high as 15,600 feet [39].

2.3. *Domestication of the laboratory mouse*

The word ‘mouse’ comes from the Latin ‘mus’ and Greek ‘mys’, both of which mean “to steal." The etymology is a reflection of mice’s ability to penetrate enclosed spaces and raid human food stores. In fact, the domestication of cats, which began with the ancient Persians and Egyptians, is believed to be directly related to the nuisance caused by mice and the attempt to safeguard human stores of food [37, 39].

House mice are ideal for domestication since they breed easily in captivity and their dietary requirements are minimal. Their constant contact with humans makes them docile, and they can be handled easily [37, 41]. An important point in the history of the domestication and development of the laboratory mouse was the predilection of the Chinese and Japanese for unusual-looking mice. Their focus was on the striking differences in the colors of their coats, which motivated breeders to select and develop

new varieties of mutant lines. This particular predilection for unique coat colors and patterns extended into the nineteenth century, when the house mouse became “an object of fancy” that spread throughout Europe, China and Japan. Experimentation of breeders with different mice to obtain new patterns was common. At the end of the nineteenth century and beginning of the twentieth century, breeders from different parts of Europe and America came up with unique names like white English sable, creamy buff, red cream, and ruby-eyed yellow as ways to mark the uniqueness of their “fancy mice” [37] [41].

The initial contact of Fanciers, as they were known, with American geneticists occurred through Miss Abbie Lathrop, a retired school teacher dedicated to the breeding of pet mice. Coincidentally, her house and farm were located close to the Bussey Institute, which was directed by William Castle of Harvard University, who was provided with fancy mice by Lathrop for early experiments in mice genetics. Lathrop bred mice from 1910 until her death in 1918, and many of the common inbred lines used today come from animals provided by Lathrop, including the C57BL/6 and C57BL/10 (commonly abbreviated as B6 and B10) [39].

2.4. *Inbred Strains of mice*

Around 1910, the investigation of the biology of cancer started with the use of inbred strains of mice. Soon after these initial experiments, inbred strains of mice were used in different types of research, such as the effect of radiation on development, constitutional disease, tissue transplantation, metabolic disturbances, neurological variations and immune responses. The great demand for these small animals introduced

the establishment and production of inbred strains with tumors for experimentation and the generations of precious mutant strains [41].

The process used to obtain a new inbred strain of mice starts with the mating (also called "outcross") of two animals or strains considered genetically dissimilar. The first offspring resulting from this mating is called “First Filial generation” (F1). Because both parents are not genetically similar to each other, the F1 siblings won’t be identical to each other, and this is always the first breeding step in a linkage analysis. The next step is the mating of two F1 siblings, and the result of this mating is called “second filial generation” (F2). The progressive mating between F2 siblings will produce F3 animals, and this process will continue. An important point that we need to remember, is that this mating needs to be done between brother and sister of each generation following the initial outcross [37, 42].

The “Committee on Standardized Genetic Nomenclature for mice” in 1989 established that a strain of mice can be considered “inbred” when it has been maintained by brother-sister mating for 20 or more consecutive generations [42, 43]. The goal of this constant mating between brother and sisters of each generation is to obtain with every subsequent filial generation a more homogeneous genotype at every locus, and this process is called inbreeding. By the end of F20, this process will have produced inbred mice that are genetically homogeneous and homozygous at all loci, except for the sex difference, and they share characteristics that uniquely set them apart from other inbred strains [37, 41]. After 20 generations, the new offspring will have reached a 98.7% inbreeding level, where the loci in the genome of each animal is more homozygous [43]. By the 30th generation, the level of heterozygosity will fall off by 19.1%, reaching a level

of 99.8% homogeneity. At 40 generations, 99.98% will be homozygous. Mice at 60 generations or higher can be considered 100% homozygous and genetically indistinguishable from all siblings and close relatives. [37, 39]

2.5. *Genealogies of inbred mouse strains*

Inbred mice are the organisms used today for modeling human disease, and we can trace their origins to the domesticated “fancy mouse.” Today, over 450 different inbred strains of mice exist, with some new strains being developed and other strains becoming extinct [41, 43].

Looking for the origin of the inbred strain, we determined that the first inbred line was DBA, developed by Clarence Cook Little in 1909, who had a predilection for genetics, biological individuality and cancer research. Over the following decade, new inbred strains were developed, such as the C57BL that came from the breeding of 57 females with 52 males; by 1918, Clarence Little, as director of the Cold Spring Harbor Laboratory, led the development of new inbred lines with his colleagues Leonell Strong and E.C. MacDawell [37, 39]. They developed the famous B6, B10, C3H, CBA, and the BALB/c. The crucial advantage of the development of these inbred lines was allowing independent researchers in different parts of the world to compare their results globally [37].

2.6. *Strains used for the research*

2.6.1. A/J inbred strain

The A/J inbred strain of mice was developed by LC Strong in the year 1921, and subsequently given to Cloudman in 1928. It is the result of a crossbreed between a

Bagg albino and an albino from Cold Spring Harbor stock, which gives its coat a white color. This strain of mice has been used in many types of research, including cancer research and in physiological and morphological studies. The A/J inbred strain is present with a moderate incidence of mammary tumors, primary lung tumors, and with relative high incidence of spontaneous cleft palate sometimes in newborns due to exposure to a variety of agents. By 1990, the A/J strain had 216 filial generations and could be considered 100% homozygous and genetically indistinguishable from all siblings and close relatives [41, 43].

2.6.2. C3H/HeJ inbred strain

The C3H/HeJ was developed by Leonell Strong (1920), and this inbred strain is a result of mating a Bagg albino female and a DBA/J male. By 1990, the inbreeding process was in the 202nd "filial generation" (F202) [41]. This inbred strain is used to conduct research of mammary tumors, hepatomas in males, and bone development [44, 45]. Previous studies determined that the C3H/HeJ reaches maximal skeletal biomechanical properties before 16 weeks of age. At this age, C3H/HeJ bone stiffness increased, but strength remained constant, work to failure decreased, and bone became more brittle [44]. A characteristic during development is nipping tails due to high density populations at the C3H/HeJ cage, without prior knowledge, the lesions developed by this practice can be confused with mousepox or rejected graft [41].

In the C3H strain, there is usually an increased bone mineral response, making it significant in the analysis of bone development. More importantly, these two

different strains of mice have often been identified as a model system for high bone mass (C3H/HeJ) and low bone mass (A/J) phenotypes, respectively[46]. The A/J mouse has a smaller condylar process than the C3H/HeJ; the anterior area of the mandible and the posterior area of the mandible are smaller in size, as well. But, A/J possesses a bigger skull length (23 mm) than C3H/HeJ (21.9 mm), and both possess the same lower jaw length (10.9 mm). The differences between these strains provide the basis for conducting research to determine the morphological differences between these two strains [47].

2.7. *Complex Traits*

There are two different types of traits in the human genome: monogenic and complex. Monogenic traits are produced by the strong influence of a single gene or allele, whereas complex traits refer to any phenotype variation with multiple contributing genes. Complex traits do not exhibit good classic Mendelian single gene recessive or dominant inheritance and are influenced by behavioral and environmental factors. [48] Although these delineations are easy to understand, they can be too simplistic; there are traits that appear to be monogenic that are influenced by variation in multiple genes and there are complex traits that can be influenced by variation in a single gene. [48].

3. THE USE OF A MOUSE MANDIBLE AS A MODEL TO STUDY DEVELOPMENT AND EVOLUTION OF COMPLEX TRAITS

Due to the detailed knowledge of the anatomy and development of the mouse mandible, it has long been used as a model for the development of complex structures. Studies using inactivation, or "knockout" of specific genes, demonstrated the effects of these genes on the development of the mandible in different parts [35, 49].

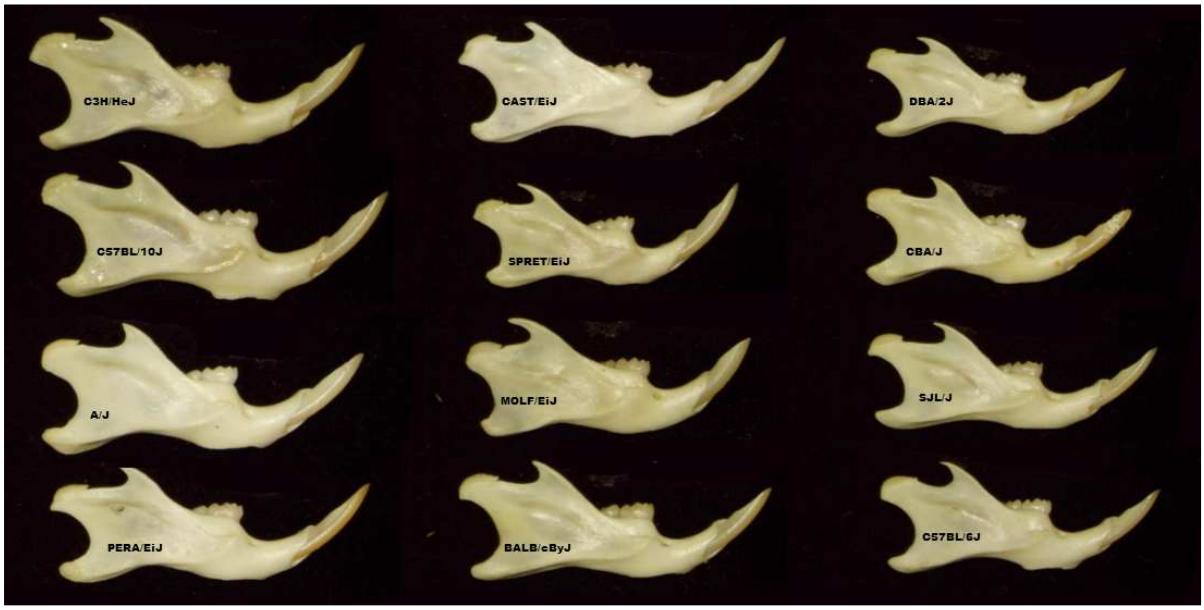

Right hemi-mandibles viewed buccally from twelve different inbred strains of mice illustrate normal variation in size, shape and microanatomy of the mandible among mice at 10 weeks of age.

Consequently, the mouse mandible has become an effective model for studying the evolution and development of complex morphological structures in humans. With the use of quantitative methods, we can analyze the effect of genes on the mandible shape. This can help us to understand more clearly the action of genes in the development and evolution of mandibular structures [50]. During the evaluation process, authors hypothesized that morphological integration results from a relationship between function

and development, and as a result of this expression, the outcome will tend to evolve together as a unit [51, 52].

Morphological integration can stem from genes, whose products are involved in the developmental process, or it can result from muscular influences as well; direct muscle influence can change the development of the mandibular process as reported by Atchley (1991) [50].

One of the first techniques used to measure the change of the mandible utilized finite element scaling, where well-known mathematical and theoretical traditions that had a long history in the engineering sciences were used. This procedure allows localization of morphological differences between forms [51, 53]. A different technique used by most geneticists evaluates the shape characteristics of the mandible in terms of the relative size; an evaluation of these parts using a series of pairwise linear distances among mandibular landmarks to characterize mandibular morphology is then performed [54].

Soon after the introduction of the geometric concept of shape, focus on features like outlines, angles, or the geometric configuration of a set of landmarks was used for the evaluation of localized morphometric variations. In order to locate quantitative trait loci (QTL) for a change of shape, which is comprised of both magnitude and direction when evaluated in three planes of space, it is necessary to combine geometric morphometric with multivariate analysis, taking into consideration all the special patterns of gene effects [49, 55].

3.1. *Embryologic Development of the Mandible*

The cells of the mandible have odontogenic, chondrogenic and skeletogenic origins. The mandible originates from neural crest cells that have their origin in the neural tube. These epithelial neural crest cells elongate and reposition organelles basally to move away from the neural tube, sending processes through the basal lamina and then transforming into mesenchymal cells. Condensation areas arise as a result of epithelial-mesenchymal interactions, which are considered to be the first signs of differentiation of the skeletal element. Once the condensations have formed, cell differentiation and morphogenesis can begin. Having undergone the epithelial-to-mesenchymal transformation, these neural cells will be the beginning of the mandibular arch, muscle and connective tissue. Therefore, the mandible is formed partially by active migration and partially by passive displacement [56, 57].

Studies done by Lee (2001) determined the existence of a Mandibular Primary Growth Center (MdPGC) that was described as, “a point of concentric radiopacity at the apical area of deciduous first molars, from which linear trabecular bones radiate to all directions of the mandible”. This growth center is important because of the morphogenetic implication of the development of the mandible and because it is a point, from which mandibular growth could be measured, based on the radiating trabeculae that eventually form the body of the mandible. Moreover, this point was also the beginning of the endochondral ossification of the condyle [57].

In the alveolar region, osteoblasts are produced by a subpopulation of cells, which generate the bony structure and odontoblasts, which then produce the teeth’s dentine. Ectomesenchyme cells also produce skeletogenic cells, which in turn produce the ramal

bone or can become chondroblasts when needed for fracture repair. Yet another population of skeletogenic cells produces osteoblasts and secondary chondroblasts that form the coronoid, condyloid and angular processes. The origin of the muscles comes from mesodermally derived mesenchyme, and these muscles influence mandibular development and growth [33, 58].

The origin source of the condyle is endochondral ossification, a process that involves numerous genes. During endochondral ossification, different gene families encode important signals that are consistent with bone formation. Both condyle and fossa contain important features that contribute to the development of the temporomandibular joint. The similarities and differences among the cells present in the chondroprogenitor layer are other issues that should be considered when deciding whether disorders develop in the early stages of jaw development or later in life [59].

3.2. *Measures of temporomandibular joint bone morphology*

The Senate Report Language for TMJ disorders urged the National Institute of Dental and Craniofacial Research (NIDCR) to work with the National Institute of Arthritis and Musculoskeletal and Skin Disease (NIAMS) and the National Institute of Biomedical Imaging and Bioengineering (NIBIB) to create measures for studying TMJ bone structure, degradation, and repair. In 1996, the NIH (National Institute of Health) Technology Assessment Conference Statement on the Diagnosis and Management of TMDs, suggested that the ideal classification system for the diagnosis of TMDs should be etiologically based rather than symptomology based [60].

The first step towards an etiology-based system was introduced in 1992 and was known as the research diagnostic criteria for temporomandibular disorders (RDC/TMD).

The RDC/TMD included the Axis I data related to physical diagnoses, primarily based on clinical signs and symptoms, and Axis II data, related to the psychological status of the patient and the pain-related disability. Imaging data are currently used in order to help differentiate disc displacement and arthralgia, osteoarthritis and osteoarthrosis. The results of the RDC/TMD validation project support this practice to enhance the Axis I physical diagnostic protocol. Hence, TMJ imaging recommendations now include computed tomography (CT) and Cone-Beam CT (CBCT) for diagnosis of osseous degenerative changes and MRI for detecting disc displacements and effusion [61].

Radiographic imaging allows evaluation of TMJ hard tissue morphology, thereby providing visualization of a wide spectrum of osseous changes due to growth, adaptive or pathologic processes. A radiographic examination of the TMJ is an essential part of diagnosis and management of TMJ diseases involving the bone supporting the articulating tissues. The growing use of medical imaging, especially RX Computed Tomography, micro-tomography and laser scanners have allowed us to reconstruct 3D images of bony structures. These virtual models and representations have generated new possibilities for quantitative analysis [62, 63]

4. MORPHOMETRIC ANALYSIS

Morphometric analysis is the statistical study of size, shape and shape changes that was applied for first time by Sir D'Arcy Thompson in the early twentieth century,

> "It can be defined as well as a collection of methods that deal directly with the coordinates of anatomical landmarks, curves or surfaces, either in two or three dimensions, rather than the traditional distance (length and width) or angle measurements" [64].

Part of its objective is to evaluate the cause and effect of the forms, and not only focus on the form [64-66].

In different animals and different fields of science, from anthropology to medicine to forensic science, the size and shape of organs have been compared during developmental stages to ensure that any defect or abnormality is identified. Many studies, such as those done by Klingenberg and Cheverud have quantified morphological differences among structures by translating, rotating and scaling to unit size specimen configurations. Those authors claim that size is distinct from shape, allowing for the separate analysis of these two components, as well as the analysis of their relationship. However, from a biological and clinical perspective, smaller or enlarged condylar sizes are indicative of variability in morphology and/or pathological processes, and size cannot be separated from shape when analyzing the TMJ [49, 51].

Precise quantitative measurements are required for characterization of TMJ morphology and longitudinal assessments; a collection of this data will capture the features of the overall form and characteristics of specific problems under study. Current quantification methods include:

4.1. *Unilateral measurements*

A research question can be answered with a single uni-dimensional measure that describes the form being studied. Measures of head circumference and wing span can give enough information to determine if an object lies within the size distribution of the population [64, 66].

4.2. *Volume measurements*

Reflect an increase or decrease in size. However, fundamental changes in specific areas are not noticeably reflected in volume measurements. Volume assessment does not reveal location and direction of proliferative or resorptive changes, which are relevant for assessment of clinical results.[67, 68] An alternative to measuring the volume is the three-dimensional coordinates of points that map the content of the closest surface in order to compare the topography or shapes evaluated.

4.3. *Landmark-based measurements*

In order to analyze the position, size and shape of a particular object or organism, we may use landmarks. These landmarks are points that locate the object in two or three dimensions of space. Using these marks can present errors related to landmark identification and oversimplified representation of the craniofacial structures [64]. A number of issues relating to the use of landmarks-based data deserve consideration; some of them are mentioned here in the order they are evaluated

i. First, it is important that the landmarks be in same way equivalent or homologous at different time points and across different subjects or specimens. Homologous structures or landmarks in this sense need to be operationally defined on the basis of their correspondence and relations. Locating 3D landmarks on complex curving structures to represent components of craniofacial form is a problem, and there is a lack of literature to provide standardization.

ii. Second, another problem relating to landmark equivalence may be encountered in developing or growing subjects, specimens or structures, such

as the TMJ condyles that undergo continuous bone remodeling throughout life. The displacement of landmarks during ontogeny results from underlying biological processes, such as subchondral growth or bone remodeling. The combination of information from these biological processes with landmark data is required to provide insight into the ontogeny of shape transformation.

iii. Third, the way in which inter-landmark distances are commonly collected is such that no attempt is made to systematically describe the relative location of landmarks, one to another. The result is a collection of measurements that may fail to describe a full 3D disposition of landmarks, as well as an over-sampling of some regions at the expense of others.

iv. Fourth, landmark–based methods leave the form between landmarks un-sampled, as no information related to curvature of the form between landmarks is preserved.

4.4. *Thin plate splines*

Thin plates are useful for comparing coordinate representations of forms to describe their changes as well as their differences. These shape changes are viewed as a deformation, and when this deformation smoothly rearranges the configuration of landmarks, we are able to estimate maximum stretch and shrinkage due to the deformation [69]. This technique estimates the difference between two objects by using a series of triangles across the morphology, connecting the homologous points and modeling the displacement of landmarks between the first (base form) and second (target form) in the x and y directions in 2D or x, y, z directions in 3D. Using pairs of linear, quadratic and cubic power surfaces (trend analysis), a type of deformable grid (thin-plate

splines) minimizes the “bending energy” required to take the first form into the second, and if the plate is completely ‘flat,’ then it has zero bending energy. A Cartesian transformation grid can be constructed using the pair of thin plate splines. The perceiving mapping does not depend on the particular coordinate system, making this a registration-free method for visualizing shape differences [69, 70].

4.5. *Finite element analysis*

Finite element analysis is used in engineering to measure the effect of loading, and it has been adapted for the mathematical comparison of forms [53, 71]. The analysis uses data derived from a set of interconnected morphological landmarks or nodes to produce a series of triangles or quadrangles. These triangles and quadrangles are 'finite elements' which become the units of morphometric analysis as defined by Richard Courant (1942). These methods are also registration-free since they provide information about the stretching of elements rather than the movements of landmarks relative to the coordinate system [51]. Finite elements have two kinds of methods: homogeneous and non-homogeneous methods.

i. Homogeneous finite element methods assume that shape changes are uniformly distributed throughout each element. This is not necessarily true of biological forms in which an element may span diverse tissue; consequently, this simplifying assumption of homogeneity may have an effect on the biological interpretation of results. It uses simple unit triangles whose apexes are equivalent landmarks between two forms. The directions of these axes indicate the directions of maximum and minimum shape changes, and their magnitudes indicate the relative measures of

these changes [64]. Moss (1988) applied the finite element analysis to the mandibles of inbred strains of mice, measuring the morphometric differences between the two forms [53].

ii. Non-homogeneous finite element methods do not assume homogeneity and use more complex elements (cubes) that allow the computation of local deformations around landmarks. Although the selection of landmarks and finite elements is largely arbitrary, the interpretation of shape changes in particular anatomical regions may differ according to element design [71].

4.6. *Biorthogonal Grids*

Developed by Bookstein, these grids provide a better numerical solution than the well-known D'Arcy Thompson transformation grids [66]. This technique computes the difference in form between two objects, one of which is designated a base form and the other which reflects shape change from the base form. Using this procedure, the whole interior of the form is taken to smoothly deform, and the matching of internal and boundary "homologies" is taken to conform to a smooth mapping of the landmarks [66]. The limitations of these analyses include the fact that the starting grid geometry may influence the interpretation of shape transformation and that different interpolations would produce different transformation grids. All of these approaches may produce different results when different landmarks are selected, and elements design will influence the outcomes of these analyses.

4.7. *Boundary/Outline, Surface and Medial Axis Morphometric Analysis*

i. Semi-landmarks or pseudo-landmarks: Several strategies exist for comparing things or organisms. One approach is to divide the outline of each organism into segments, each of which can be imagined as being delimited by pseudo landmarks. Such pseudo landmarks are operationally, but not necessarily biologically, equivalent to either an evolutionary or developmental sense [66].

ii. Curves: Analysis of curves for statistical interpretation, especially analysis of 3-D structures, comes with many challenges. Comparisons of curves can be made as functions if curves are open, but for closed surfaces, different approaches include tangent angles to points in the outline. These points need to represent operational homologies, be spaced equidistantly around an outline, or represent nodes of the outline divided into equal numbers of segments [66, 72].

iii. Outline/Surface and Medial representation: Medial representation, introduced by Blum in 1967, defines shape by a symmetric axis or skeleton that consists of all points within a form that do not have a unique nearest boundary point upon the shape. Associated with each point on the symmetric axis is a width function defining the distance to any of the set of equally distant nearest boundary points [73]. Even though the use of medial representation as the basis for the identification of operationally homologous structures is a strategy for comparison of forms with limited external landmarks, it should be noted that different algorithms to

determine the medial axis representation and subtle differences in outline form may result in quite different topologies. Since the medial representation models are based on coarse grids of the medial axis, the shape analysis captures only large scale shape differences, whereas surface shape analysis captures both small and large scale shape differences [64].

4.8. *Surface Models*

i. Closest Point measurements between the surfaces can display changes with color maps. However, the Closest Point method measures the closest distances, not corresponding distances, between anatomical points on two or more longitudinally obtained images. For this reason, Closest Point measurements fail to quantify large changes in bone during disease progression in a given patient and differences in morphology between individuals [74].

ii. Shape correspondence: SPHARM-PDM (spherical harmonics-point distributed models) software was developed as part of the National Alliance of Medical Image Computing (NA-MIC, NIH Roadmap for Medical Research) and has been adapted for use with CBCT imaging of the craniofacial complex [75]. Shape analysis is up and coming in the medical community because of its potential to precisely locates morphological changes between healthy and pathological structures. SPHARM-PDM is a tool that computes point-based models using a parametric boundary description for the computing of shape analysis [67]. The 3D virtual surface models are converted into a corresponding

spherical harmonic description (SPHARM), which is then sampled into triangulated surfaces (SPHARM-PDM) [74]. These results are better than those obtained using Closest Point (CP) correspondence-based analysis. This standard analysis is currently used by most software systems, but its limitations are that is does not map surfaces based on anatomical geometry and it usually underestimates rotational and large translational movements. For example, in the assessment of surgical outcomes, CP color maps measure surgical jaw displacement as the smallest separation between the boundaries of the same structure, which may not be the correct anatomical corresponding boundaries on anatomical structures pre- and post-surgery[67, 75].

5. IMAGE ANALYSIS PROCEDURES

Storage, handling and sharing of imaging data has been standardized as Digital Imaging and Communications in Medicine (DICOM) format that can be read by multiple open source and commercial image analysis software [76]. ITK-SNAP is a software application that allows users to read, navigate and construct surface models defined as segments from a stack of cross-sectional slices of a three-dimensional medical image volume. The significance of the segmentation process is that it allows conclusive interpretation of 3D morphology [77]. 3D virtual surface models should be built from isotropic 0.02 x 0.02 x 0.02 mm voxels of a set of more than 500 axial cross-sectional slices for each volume, in order to produce 3D models that are usable for shape analysis. The SPHARM-PDM software is used to convert the 3D virtual surface models into a

corresponding spherical harmonic description, which is then sampled into triangulated surfaces [78].

In addition, the differences in the models are visually and statistically assessed using various mapping techniques from each individual in the population to the sample mean. These mapping techniques are the vector mapping technique and distance mapping. Vector maps provide visualization of displacement between paired correspondent point-based models indicating the magnitude of displacement (expansion or contraction might show depending on the direction of the vector), and distance color maps visualize displacements and localize regions of surface remodeling [79].

A multivariate analysis of covariance is commonly used to calculate and compare the mean group morphology model between the two different strains of A/J and C3H mice. P-value maps for the testing group's differences are calculated based on the Hotelling T2 metric, based on covariance matrices. Pearson correlation coefficients and their P values compute between individuals global and local morphological variation. Since the scans develop a 3D image, all sides of the mandibular bone are easily viewed and for this reason, any inconsistencies in the bone formation in relation to the ramus or condyle are highlighted for further analysis.

5.1. *Micro-CT Technology*

In the early 1980s, the first micro-CT scanners were developed using bench-top X-ray CT sources. Feldkamp and Davis advanced from the fan beam to one beam geometry in the late 1980s. The current phase of micro-CT development involves bench-top scanners that can scan small animals and is used for drug discovery, cancer detection and monitoring. [80].

The micro-CT has recently become the “gold standard’’ for evaluation of bone morphology and micro architecture in mice and other small animal models. Currently available micro CT scanners can provide images of live rodent organs at spatial resolutions from cellular (20 µm) down to sub cellular dimensions (1 µm) and fill the resolution-hiatus between microscope imaging and mini-CT imaging of intact volumes [80].

This scanner can achieve an isotropic voxel size as low as a few micrometers, which is sufficiently small enough to investigate structures such as mouse trabeculae that have widths of approximately 30 to 50 µm. Typically, voxel sizes from micro CT images have three equal dimensions and therefore are described as isotropic voxels. Ideally, the smallest voxel size available would be used for all scans; however, this would require longer acquisition times to collect more projections and generate large data sets. Consequently, the tradeoff between voxel size and scan time should be carefully considered. In the case of live animals, such as mice, it is almost impossible to obtain the real volume of a bone because scanning time (radiation load) of living tissues should be as short as possible to limit radiation doses absorbed by living tissue during the process of exposure.

There are several advantages of using micro-CT for assessment of bone morphology in different specimens, including mice. It allows for effective 3D measurement of trabecular morphology and volume, as well as thickness and separation, as opposed to inferring these values based on 2D stereologic models, as is done with standard histologic evaluations [81]. Compared with 2D histology, a significantly larger volume of interest is analyzed, and measurement scans can be performed at a much faster

rate than typical histologic analyses of histomorphometrical parameters using decalcified bone specimens. Furthermore, assessment of bone morphology by micro CT scanning is non-destructive; therefore, samples can be used subsequently for other assays, such as histologic or mechanical testing. The first study using micro-CT was an examination of subchondral bone changes in a guinea pig model of osteoarthritis. Since that time, micro-CT has been used for a wide range of studies of bone mass and bone morphology, including analysis of growth and development of skeletal phenotypes of different genetically altered mouse strains and animal models used for the study of osteoporosis [82-84].

In summary, TMDs have become a common condition with very high treatment costs. The etiology of TMD is multifactorial, and there exists controversy among authors regarding its different possible causes. TMD is more prevalent in women than in men, and there are approximately 5.3 million Americans currently seeking treatment for this condition. Mouse models have been recognized as useful for the study of this abnormality because mice are genetically very similar to humans.

In order to understand TMD, we need to first understand the normal anatomy of the condyle. To this end, morphometric analysis is useful for the statistical analysis of changes to the size and shape of the condyle over time. This analysis is up and coming in the medical community because of its potential to precisely locate morphological changes in healthy and pathological structures, and it has also been validated in several studies. In order to study small structures such as the condyle, the use of the micro-CT is advisable because it is considered the “gold standard’’ for the evaluation of bone morphology and microarchitecture in mice and other small animal models. Micro-CT scanners provide

images at spatial resolutions of cellular (20 µm) to subcellular dimensions (1 µm), and provide the best data for the evaluation of the condylar microstructure.

Our long-term goal is to integrate morphology, size, and genetic information from the mandibular condyle, and correlate it with normal occlusion and/or malocclusion during growth to identify polymorphisms in genetic factors that underlie the differences in anatomical morphologies, both within and between common isogenic strains.

REFERENCES

1. Alexiou, K., H. Stamatakis, and K. Tsiklakis, *Evaluation of the severity of temporomandibular joint osteoarthritic changes related to age using cone beam computed tomography.* Dentomaxillofac Radiol, 2009. **38**(3): p. 141-7.

2. Alomar, X., J. Medrano, J. Cabratosa, J.A. Clavero, M. Lorente, I. Serra, J.M. Monill, and A. Salvador, *Anatomy of the Temporomandibular Joint.* Seminars in Ultrasound, CT and MRI, 2007. **28**(3): p. 170-183.

3. LeResche, L., L.A. Mancl, M.T. Drangsholt, G. Huang, and M. Von Korff, *Predictors of onset of facial pain and temporomandibular disorders in early adolescence.* Pain, 2007. **129**(3): p. 269-78.

4. Merida-Velasco, J.R., J.F. Rodriguez-Vazquez, J.A. Merida-Velasco, I. Sanchez-Montesinos, J. Espin-Ferra, and J. Jimenez-Collado, *Development of the human temporomandibular joint.* The Anatomical record, 1999. **255**(1): p. 20-33.

5. Bernard, J.P., *The Anatomical Basis of Dentistry*. 3rd Edition. ed2001, St. Louis: Mosby.

6. Shibukawa, Y., B. Young, C. Wu, S. Yamada, F. Long, M. Pacifici, and E. Koyama, *Temporomandibular joint formation and condyle growth require Indian hedgehog signaling.* Dev Dyn, 2007. **236**(2): p. 426-34.

7. Ohno, S., T. Schmid, Y. Tanne, T. Kamiya, K. Honda, M. Ohno-Nakahara, N. Swentko, T.A. Desai, K. Tanne, C.B. Knudson, and W. Knudson, *Expression of superficial zone protein in mandibular condyle cartilage.* Osteoarthritis and cartilage / OARS, Osteoarthritis Research Society, 2006. **14**(8): p. 807-13.

8. Mew, J.R., *The aetiology of temporomandibular disorders: a philosophical overview.* European journal of orthodontics, 1997. **19**(3): p. 249-58.

9. Sale, H. and A. Isberg, *Delayed temporomandibular joint pain and dysfunction induced by whiplash trauma: a controlled prospective study.* J Am Dent Assoc, 2007. **138**(8): p. 1084-91.

10. Cevidanes, L.H., A.K. Hajati, B. Paniagua, P.F. Lim, D.G. Walker, G. Palconet, A.G. Nackley, M. Styner, J.B. Ludlow, H. Zhu, and C. Phillips, *Quantification of condylar resorption in temporomandibular joint osteoarthritis.* Oral Surg Oral Med Oral Pathol Oral Radiol Endod, 2010. **110**(1): p. 110-7.

11. Mutlu, N., M.E. Erdal, H. Herken, G. Oz, and Y.A. Bayazit, *T102C polymorphism of the 5-HT2A receptor gene may be associated with temporomandibular dysfunction.* Oral Diseases, 2004. **10**(6): p. 349-352.

12. Buescher, J.J., *Temporomandibular joint disorders.* Am Fam Physician, 2007. **76**(10): p. 1477-82.

13. Seligman, D.A., A.G. Pullinger, and W.K. Solberg, *The Prevalence of Dental Attrition and Its Association with Factors of Age, Gender, Occlusion, and Tmj Symptomatology.* Journal of Dental Research, 1988. **67**(10): p. 1323-1333.

14. Rodrigues, J.H., D.A. Biasotto-Gonzalez, S.K. Bussadori, R.A. Mesquita-Ferrari, K.P. Fernandes, C.A. Tenis, and M.D. Martins, *Signs and symptoms of temporomandibular disorders and their impact on psychosocial status in non-patient university student's population.* Physiother Res Int, 2010.

15. Helenius, L.M., D. Hallikainen, I. Helenius, J.H. Meurman, M. Kononen, M. Leirisalo-Repo, and C. Lindqvist, *Clinical and radiographic findings of the temporomandibular joint in patients with various rheumatic diseases. A case-control study.* Oral surgery, oral medicine, oral pathology, oral radiology, and endodontics, 2005. **99**(4): p. 455-63.

16. Yura, S., K. Ooi, S. Kadowaki, Y. Totsuka, and N. Inoue, *Magnetic resonance imaging of the temporomandibular joint in patients with skeletal open bite and subjects with no dentofacial abnormalities.* The British journal of oral & maxillofacial surgery, 2010. **48**(6): p. 459-61.

17. Wiese, M., A. Wenzel, H. Hintze, A. Petersson, K. Knutsson, M. Bakke, T. List, and P. Svensson, *Osseous changes and condyle position in TMJ tomograms: impact of RDC/TMD clinical diagnoses on agreement between expected and actual findings.* Oral surgery, oral medicine, oral pathology, oral radiology, and endodontics, 2008. **106**(2): p. e52-63.

18. Von Korff, M.R., J.A. Howard, E.L. Truelove, E. Sommers, E.H. Wagner, and S. Dworkin, *Temporomandibular disorders: variation in clinical practice.* Medical care, 1988: p. 307-314.

19. Dworkin, S.F. and L. LeResche, *Research diagnostic criteria for temporomandibular disorders: review, criteria, examinations and specifications, critique.* Journal of craniomandibular disorders : facial & oral pain, 1992. **6**(4): p. 301-55.

20. Nilsson, I.M., T. List, and M. Drangsholt, *Prevalence of temporomandibular pain and subsequent dental treatment in Swedish adolescents.* J Orofac Pain, 2005. **19**(2): p. 144-50.

21. Helkimo, M., *Epidemiological surveys of dysfunction of the masticatory system.* Oral sciences reviews, 1976. **7**: p. 54-69.

22. Magnusson, T., I. Egermark, and G.E. Carlsson, *A longitudinal epidemiologic study of signs and symptoms of temporomandibular disorders from 15 to 35 years of age.* Journal of orofacial pain, 2000. **14**(4): p. 310-9.

23. LeResche, L., L. Mancl, J.J. Sherman, B. Gandara, and S.F. Dworkin, *Changes in temporomandibular pain and other symptoms across the menstrual cycle.* Pain, 2003. **106**(3): p. 253-61.

24. Locker, D. and G. Slade, *Prevalence of symptoms associated with temporomandibular disorders in a Canadian population.* Community Dent Oral Epidemiol, 1988. **16**(5): p. 310-3.

25. Bouvier, M. and W.L. Hylander, *Effect of bone strain on cortical bone structure in macaques (Macaca mulatta).* Journal of morphology, 1981. **167**(1): p. 1-12.

26. Tuominen, M., T. Kantomaa, and P. Pirttiniemi, *Effect of food consistency on the shape of the articular eminence and the mandible. An experimental study on the rabbit.* Acta odontologica Scandinavica, 1993. **51**(2): p. 65-72.

27. Yamada, K. and D.B. Kimmel, *The effect of dietary consistency on bone mass and turnover in the growing rat mandible.* Archives of Oral Biology, 1991. **36**(2): p. 129-38.

28. Boyd, R.L., C.H. Gibbs, P.E. Mahan, A.F. Richmond, and J.L. Laskin, *Temporomandibular joint forces measured at the condyle of Macaca arctoides.* American journal of orthodontics and dentofacial orthopedics : official publication of the American Association of Orthodontists, its constituent societies, and the American Board of Orthodontics, 1990. **97**(6): p. 472-9.

29. Pirttiniemi, P., T. Kantomaa, and T. Sorsa, *Effect of decreased loading on the metabolic activity of the mandibular condylar cartilage in the rat.* European journal of orthodontics, 2004. **26**(1): p. 1-5.

30. Bouvier, M., *Effects of age on the ability of the rat temporomandibular joint to respond to changing functional demands.* Journal of Dental Research, 1988. **67**(9): p. 1206-12.

31. Chen, J., K.P. Sorensen, T. Gupta, T. Kilts, M. Young, and S. Wadhwa, *Altered functional loading causes differential effects in the subchondral bone and condylar cartilage in the temporomandibular joint from young mice.* Osteoarthritis and Cartilage, 2009. **17**(3): p. 354-361.

32. Mina, M., *Regulation of mandibular growth and morphogenesis.* Critical reviews in oral biology and medicine : an official publication of the American Association of Oral Biologists, 2001. **12**(4): p. 276-300.

33. Cobourne, M.T. and P.T. Sharpe, *Tooth and jaw: molecular mechanisms of patterning in the first branchial arch.* Archives of Oral Biology, 2003. **48**(1): p. 1-14.

34. Purcell, P., B.W. Joo, J.K. Hu, P.V. Tran, M.L. Calicchio, D.J. O'Connell, R.L. Maas, and C.J. Tabin, *Temporomandibular joint formation requires two distinct hedgehog-dependent steps.* Proc Natl Acad Sci U S A, 2009. **106**(43): p. 18297-302.

35. Purcell, P., A. Jheon, M.P. Vivero, H. Rahimi, A. Joo, and O.D. Klein, *Spry1 and spry2 are essential for development of the temporomandibular joint.* Journal of Dental Research, 2012. **91**(4): p. 387-93.

36. Scafoglieri, A., P. Van Roy, and J.P. Clarijs, *[Left-right asymmetries and other common anatomical variants of temporomandibular articular surfaces]*. Nederlands tijdschrift voor tandheelkunde, 2008. **115**(1): p. 14-21.

37. Silver, L.M., *Mouse Genetics* - in *Oxford University Press*1995.

38. Hedrich, H., *The Laboratory Mouse* ed. S. edition2012.

39. Morse, H.C., *Origins of Inbred mice*1978, Maine.

40. Gama Sosa, M.A., R. De Gasperi, and G.A. Elder, *Animal transgenesis: an overview.* Brain Struct Funct, 2010. **214**(2-3): p. 91-109.

41. JacksonLaboratory, T., *Handbook on Genetically Standardized JAX Mice*. Four Edition ed1991.

42. Guénet, J.L. and F.J. Benavides, *Mouse strains and genetic nomenclature.* 2011.

43. Beck, J.A., S. Lloyd, M. Hafezparast, M. Lennon-Pierce, J.T. Eppig, M.F.W. Festing, and E.M.C. Fisher, *Genealogies of mouse inbred strains.* Nature Genetics, 2000. **24**(1): p. 23-+.

44. Voide, R., G.H. van Lenthe, and R. Müller, *Differential Effects of Bone Structural and Material Properties on Bone Competence in C57BL/6 and C3H/He Inbred Strains of Mice.* Calcified Tissue International, 2008. **83**(1): p. 61-69.

45. Everett, E.T., *Fluoride's Effects on the Formation of Teeth and Bones, and the Influence of Genetics.* J Dent Res, 2011. **90**(5): p. 552-60.

46. Ng, A.H., S.X. Wang, C.H. Turner, W.G. Beamer, and M.D. Grynpas, *Bone quality and bone strength in BXH recombinant inbred mice.* Calcified Tissue International, 2007. **81**(3): p. 215-23.

47. Everett, E., *Craniofacial morphology of 14 inbred strains of mice. MPD:Everett1*., in *Mouse Phenome Database web site* May, 2011., The Jackson Laboratory, Bar Harbor, Maine USA.

48. Lander, E.S. and N.J. Schork, *Genetic dissection of complex traits.* Science, 1994. **265**(5181): p. 2037-48.

49. Klingenberg, C.P., L.J. Leamy, E.J. Routman, and J.M. Cheverud, *Genetic architecture of mandible shape in mice: effects of quantitative trait loci analyzed by geometric morphometrics.* Genetics, 2001. **157**(2): p. 785-802.

50. Atchley, W.R. and B.K. Hall, *A model for development and evolution of complex morphological structures.* Biological reviews of the Cambridge Philosophical Society, 1991. **66**(2): p. 101-57.

51. Cheverud, J.M., S.E. Hartman, J.T. Richtsmeier, and W.R. Atchley, *A quantitative genetic analysis of localized morphology in mandibles of inbred mice using finite element scaling analysis.* J Craniofac Genet Dev Biol, 1991. **11**(3): p. 122-37.

52. Klingenberg, C.P., *Morphological integration and developmental modularity.* Annual review of ecology, evolution, and systematics, 2008. **39**: p. 115-132.

53. Moss, M., *Finite element method comparison of murine mandibular form differences.* J Craniofac Genet Dev Biol, 1988. **8**: p. 3-20.

54. Atchley, W.R., A.A. Plummer, and B. Riska, *Genetic analysis of size-scaling patterns in the mouse mandible.* Genetics, 1985. **111**(3): p. 579-595.

55. Duarte, L.C., L.R. Monteiro, F.J. Von Zuben, and S.F. Dos Reis, *Variation in mandible shape in Thrichomys apereoides (Mammalia: Rodentia): geometric analysis of a complex morphological structure.* Syst Biol, 2000. **49**(3): p. 563-78.

56. Smith, R.J. and J. Frommer, *Condylar growth gradients: possible mechanism for spiral or arcial growth of the mandible.* Angle Orthod, 1980. **50**(4): p. 274-8.

57. Lee, S.K., Y.S. Kim, H.S. Oh, K.H. Yang, E.C. Kim, and J.G. Chi, *Prenatal development of the human mandible.* The Anatomical record, 2001. **263**(3): p. 314-25.

58. Atchley, W.R., A.A. Plummer, and B. Riska, *Genetics of mandible form in the mouse.* Genetics, 1985. **111**(3): p. 555-77.

59. Kinumatsu, T., Y. Shibukawa, T. Yasuda, M. Nagayama, S. Yamada, R. Serra, M. Pacifici, and E. Koyama, *TMJ development and growth require primary cilia function.* Journal of Dental Research, 2011. **90**(8): p. 988-94.

60. Anderson, G.C., Y.M. Gonzalez, R. Ohrbach, E.L. Truelove, E. Sommers, J.O. Look, and E.L. Schiffman, *The Research Diagnostic Criteria for Temporomandibular Disorders. VI: future directions.* Journal of orofacial pain, 2010. **24**(1): p. 79-88.

61. Ahmad, M., L. Hollender, Q. Anderson, K. Kartha, R. Ohrbach, E.L. Truelove, M.T. John, and E.L. Schiffman, *Research diagnostic criteria for temporomandibular disorders (RDC/TMD): development of image analysis criteria and examiner reliability for image analysis.* Oral surgery, oral medicine, oral pathology, oral radiology, and endodontics, 2009. **107**(6): p. 844-60.

62. Borah, B., G.J. Gross, T.E. Dufresne, T.S. Smith, M.D. Cockman, P.A. Chmielewski, M.W. Lundy, J.R. Hartke, and E.W. Sod, *Three-dimensional microimaging (MRmicroI and microCT), finite element modeling, and rapid prototyping provide unique insights into bone architecture in osteoporosis.* Anat Rec, 2001. **265**(2): p. 101-10.

63. Bouxsein, M.L., S.K. Boyd, B.A. Christiansen, R.E. Guldberg, K.J. Jepsen, and R. Müller, *Guidelines for assessment of bone microstructure in rodents using micro-computed tomography.* Journal of Bone and Mineral Research, 2010. **25**(7): p. 1468-1486.

64. Bookstein, F.L., *Morphometric Tools for Landmark Data Geometry and Biology*. First Paperback Edition 1997 ed1991: Cambridge University Press.

65. Klingenberg, C. and L. Monteiro, *Distances and Directions in Multidimensional Shape Spaces: Implications for Morphometric Applications.* Systematic Biology, 2005. **54**(4): p. 678-688.

66. Lestrel, P.E., *Morphometrics for the life sciences*. Vol. 7. 2000: World Scientific Publishing Company Incorporated.

67. Styner, M., I. Oguz, S. Xu, C. Brechbuhler, D. Pantazis, J.J. Levitt, M.E. Shenton, and G. Gerig, *Framework for the Statistical Shape Analysis of Brain Structures using SPHARM-PDM.* The insight journal, 2006(1071): p. 242-250.

68. Saccucci, M., A. Polimeni, F. Festa, and S. Tecco, *Do skeletal cephalometric characteristics correlate with condylar volume, surface and shape? A 3D analysis.* Head & face medicine, 2012. **8**(1): p. 15.

69. Franchi, L., T. Baccetti, and J.A. McNamara, Jr., *Thin-plate spline analysis of mandibular growth.* The Angle orthodontist, 2001. **71**(2): p. 83-9.

70. Rosas, A. and M. Bastir, *Thin-plate spline analysis of allometry and sexual dimorphism in the human craniofacial complex.* American journal of physical anthropology, 2002. **117**(3): p. 236-45.

71. Richtsmeier, J.T. and J.M. Cheverud, *Finite element scaling analysis of human craniofacial growth.* Journal of craniofacial genetics and developmental biology, 1986. **6**(3): p. 289-323.

72. Bookstein, F.L., *Morphometric tools for landmark data: geometry and biology*1997: Cambridge University Press.

73. Bookstein, F.L., *Linear machinery for morphological distortion.* Computers and biomedical research, an international journal, 1978. **11**(5): p. 435-58.

74. Gerig, G., M. Styner, D. Jones, D. Weinberger, and J. Lieberman. *Shape analysis of brain ventricles using spharm*. in *Mathematical Methods in Biomedical Image Analysis, 2001. MMBIA 2001. IEEE Workshop on*. 2001. IEEE.

75. Paniagua, B., L. Cevidanes, H. Zhu, and M. Styner, *Outcome quantification using SPHARM-PDM toolbox in orthognathic surgery.* International Journal of Computer Assisted Radiology and Surgery, 2010.

76. Mildenberger, P., M. Eichelberg, and E. Martin, *Introduction to the DICOM standard.* European radiology, 2002. **12**(4): p. 920-7.

77. Yushkevich, P.A., J. Piven, H.C. Hazlett, R.G. Smith, S. Ho, J.C. Gee, and G. Gerig, *User-guided 3D active contour segmentation of anatomical structures: significantly improved efficiency and reliability.* Neuroimage, 2006. **31**(3): p. 1116-28.

78. Paniagua, B., L. Cevidanes, D. Walker, H. Zhu, R. Guo, and M. Styner, *Clinical application of SPHARM-PDM to quantify temporomandibular joint osteoarthritis.* Computerized Medical Imaging and Graphics, 2010.

79. AlHadidi, A., L.H. Cevidanes, B. Paniagua, R. Cook, F. Festy, and D. Tyndall, *3D quantification of mandibular asymmetry using the SPHARM-PDM tool box.* International Journal of Computer Assisted Radiology and Surgery, 2012. **7**(2): p. 265-271.

80. Feldkamp, L.A., S.A. Goldstein, A.M. Parfitt, G. Jesion, and M. Kleerekoper, *The direct examination of three-dimensional bone architecture in vitro by computed tomography.* J Bone Miner Res, 1989. **4**(1): p. 3-11.

81. Muller, R., H. Van Campenhout, B. Van Damme, G. Van Der Perre, J. Dequeker, T. Hildebrand, and P. Ruegsegger, *Morphometric analysis of human bone biopsies: a quantitative structural comparison of histological sections and micro-computed tomography.* Bone, 1998. **23**(1): p. 59-66.

82. Layton, M.W., S.A. Goldstein, R.W. Goulet, L.A. Feldkamp, D.J. Kubinski, and G.G. Bole, *Examination of subchondral bone architecture in experimental*

osteoarthritis by microscopic computed axial tomography. Arthritis and rheumatism, 1988. **31**(11): p. 1400-5.

83. Enomoto, A., J. Watahiki, T. Yamaguchi, T. Irie, T. Tachikawa, and K. Maki, *Effects of mastication on mandibular growth evaluated by microcomputed tomography.* The European Journal of Orthodontics, 2009. **32**(1): p. 66-70.

84. Fajardo, R.J. and R. Muller, *Three-dimensional analysis of nonhuman primate trabecular architecture using micro-computed tomography.* American Journal of Physical Anthropology, 2001. **115**(4): p. 327-336.

II. MANUSCRIPT

INTRODUCTION

Mouse models are increasingly recognized as powerful tools for medical research due to their genetic similarity to humans, which makes them very effective for the study of human diseases. Mice are among the smallest mammals known, with a short gestation time and females that prolifically breed in a laboratory environment [1].

The size and shape of the mouse mandible are highly heritable quantitative traits that are sufficiently variable to allow identification of differences between inbred mouse strains [2, 3]. Moreover, many studies have revealed that mouse strain identification can be reliably accomplished by means of discriminant analysis using mandible measurements [4]. A comprehensive analysis of the mandibular condyle using different strains of mice would provide the necessary information for understanding possible anomalies in the mandible. The contribution of the temporomandibular joint (TMJ) and its condyle to the development of the mandible is significantly related to the development of TMJ disorders (TMDs) [5]. In addition, previous studies have recognized that environmental factors, such as transverse abnormality and forced bites (bruxism), as well as increasing age, correlate with an increased risk of developing TMDs [6]. In order to detect these sizes and shape disorders, it is important to become familiar with the normal appearance of the condyle in cross-sectional diagnostic images. This detailed characterization of the condylar articular surface may be important in determining the

precise cause of these disorders, while taking into consideration the fact that mandibular condyles experience changes in size and shape during early growth and development [7-9]. Hence, the development and progression of TMD in humans is multifactorial and complex; using the mouse model to characterize mandibular morphology may provide clues to understand TMD pathology.

TMDs are reported to occur in up to 75% of adults who show at least one sign of joint dysfunction upon examination, which may include clicking, facial pain, development of a progressive anterior open bite and limitation or deviation of jaw movements [5, 7, 8, 10, 14]. However, only approximately 5% of adults with TMJ symptoms require treatment and develop chronic or debilitating symptoms [10]. The complex etiology associated with TMDs are cited to be due to a history of trauma [11], systemic diseases like juvenile idiopathic arthritis, developmental abnormalities during growth, and psychological stress [9, 12, 13]. This complex and multifactorial disorder can be best investigated through studies of the mandibular condyle. Accordingly, the mouse model provides an ideal system to investigate condylar morphological variation and therefore development.

Since the mouse mandibular condyle is a small anatomical structure, microtomography (micro-CT) is considered the ‘‘gold standard’’ for the evaluation of bone morphology and microarchitecture in small animal models [15]. Two-dimensional (2D) and three-dimensional (3D) morphological measurements using micro-CT highly correlate with those from histomorphometry [16, 17]. The adaptation of bone to its hormonal and mechanical environments can only be fully understood in terms of its 3D

architecture, which links altered bone cell function, mechanical properties, and load-bearing functions of the skeleton [18].

The goals of this pilot study were as follows: I) To compare morphological differences in mandibular condyles in different inbred strains of mice (AJ and C3H/HeJ) with the same genetic background, and in varying age groups (3-5 weeks, 6-8 weeks, and 9-11 weeks) by quantifying the articulating surface of the mandibular condyle bilaterally (right and left); II) To compare morphological differences in the mandibular condyle between the two inbred strains of mice, by comparing the articulating surfaces of the condyle of the mandible between two different inbred strains of mice (AJ and C3H/HeJ) at ages 3-5 weeks, 6-8 weeks and 9-11 weeks; III) To qualitatively determine which part of the condylar articular surface is more stable and less susceptible to morphologic variability within each mouse strain and age group.

The long-term goal of this study is to integrate morphology, size, and genetic information from the mandibular condyle, and correlate it with normal occlusion and/or malocclusion during growth to identify genetic polymorphisms that underlie differences in anatomical morphologies, both within and between common isogenic strains. The identification of genes that play a role in the development of the condyle and other structures of the mandible may help us better understand how these structures change over time, thereby opening the possibility for further investigation of gene-related anomalies of the mandibular condyle.

MATERIALS AND METHODS

Animal tissues

Tissues were removed from the intact skulls of male mice from two inbred strains; namely, A/J (n= 27) and C3H/HeJ (n= 27). The heads were from mice 3-5 weeks (n=6 per strain), 6-8 weeks (n=6 per strain), and 9-11 weeks (n=15 per strain) of age.

Micro-CT

Mouse skulls dissected of fur were placed in a custom carrier for micro-CT scanning using a Skyscan 1074HR portable micro-CT scanner (Skyscan, Aartselaar, Belgium). Image pixel size following reconstructions = 20.7 micrometers; X-ray detector 768x576 pixels 8-bit x-ray camera; x-ray source 20-40 kV / 0-1000 microAmp. Samples were scanned under standard conditions (40kV and 1000 microAmp; exposure = 420 milliseconds; object to source (mm) = 182.83; rotation angle 180 degrees at 0.9 degree steps; 16bit TIFF images collected). Reconstructions were performed using NRecon (Version: 1.4; Skyscan), which is based on the Feldkamp algorithm, and which was used under standard settings (optimal post alignment to correct for pixel shift, smoothing = 1, ring artifact correction = 20, and beam hardening correction = 60%).

Image acquisition and segmentation

Micro-CT scans obtained were converted to Digital Imaging and Communications in Medicine (DICOM) files/images. These images were subsequently converted to Guys Image Processing Lab (GIPL) format for 3D visualization using ITK-SNAP open source software [19]. 3D virtual surface models were built from a set of more than 500 axial cross-sectional slices for each image, with images reformatted from isotropic voxels of 0.02 x 0.02 x 0.02 mm. The construction of virtual surface models from micro-CT cross-

sectional slices is a semi-automatic process called segmentation, which was performed with ITK-SNAP software. For each mouse, the mandibular condyle was selected as the anatomical region of interest (ROI) to construct the surface models. Specifically, the ROI was the condylar articular surface that was defined by cropping the condyle to a plane perpendicular to the condylar long axis, passing immediately below the anterior and posterior poles of the condyle. The condylar surface models were registered using 3D Slicer software (open-source software, www.slicer.org); the registration of all condyles in the same coordinate system aimed to approximate condyles of all mice prior to computation of shape correspondence with Spherical Harmonic_ Point Distribution Model (SPHARM_PDM) [20].

Segment pre-processing

Before computing the shapes, pre-processing of anatomical segments were assured with the following steps. First, since virtual cropping of the 3D model left open segments, these interior holes were filled in order to preserve the spherical topology needed for SPHARM-PDM shape analysis. Second, in order to avoid the appearance of a block-like image with "staircase" edges, a smoothing procedure was applied. Lastly, binary segmentation volumes were created from the surfaces.

SPHARM-PDM computing

The SPHARM-PDM shape analysis software processes binary segmentation volumes to ensure spherical topology, which are then converted to surface meshes. Next, the spherical parametrization is computed from the surface meshes using area–preserving, distortion-minimizing spherical mapping. The SPHARM description is computed from the mesh and its spherical parametrization [21]. This description is then

sampled into triangular surfaces (SPHARM-PDM) via an icosahedron subdivision of the spherical parametrization (Figure 1).

Analysis of morphological differences

The SPHARM-PDM toolbox is a shape correspondence software package that computes point-based models such that each of the 4002 points in a condyle model corresponds in all 54 mice. These corresponding point-based models were used to compute a composite average model for each strain in each age group. This procedure allowed three distinct types of evaluations for each of the three study aims that were previously described.

Comparison of average group morphologies between different age groups within and between strains

Twelve composite average surface models, one for each age group (3 age groups), each strain (2 strains), and each side (right and left condyles) were computed (Figure 2). The composite average models of 6-8 weeks were subtracted from models of 3-5 weeks, models of 9-11 weeks were subtracted from models of 3-5 weeks, and models of 9-11 weeks were subtracted from models of 6-8 weeks for each strain and side. The subtraction of each average model generated different vectors, absolute distance maps, and signed distance maps that were visually and statistically tested for differences between age groups. Vector maps provided the differences between paired correspondent point-based models, indicating the magnitude, location, and direction of morphological variations between different age groups. The signed distances measured the size and direction of each vector at the 4002 corresponding points, and quantified differences in the following condylar articular surface regions: anterior, antero-superior, postero-superior, posterior, antero-medial, postero-medial, antero-lateral, and postero-lateral.

Comparison of average group morphology between different strains in the same age group

The twelve composite average models computed in Aim I were used for comparisons of morphological differences between the strains. Composite average models for the C3H strain were subtracted from AJ composite average models in each age group and side; the subtraction of each average model generated different vectors, absolute distance maps, and signed distance maps that were visually and statistically tested for differences between strains. Vector maps provided differences between paired correspondent point-based models, indicating the magnitude, location and direction of morphological variation between groups. The signed distances measured the size and direction of each vector at the 4002 corresponding points and quantified differences in the following condylar articular regions: anterior, antero-superior, postero-superior, posterior, antero-medial, postero-medial, antero-lateral, and postero-lateral.

Comparison of individual morphology within each age group and strain

Each individual condylar point–based model was compared to the composite average model for its group. Each individual model was subtracted from its group composite average, generating individual different vectors that were visually and qualitatively evaluated to determine the morphological variability of each mouse compared to its group composite average, and to assess anatomical areas that were more stable and less susceptible to morphologic variability. Even though these maps can also provide quantitative information, because this study did not use any scaling to compensate for size differences, quantitative measurements of individual variability would be confounded by size differences.

Statistical analysis

Multivariate analysis of covariance (MANCOVA) was used to test whether average group morphology models were different when compared to morphologies in the three age groups (Aim I) and between A/J and C3H/HeJ mouse strains (Aim II). P-values for differences between groups were calculated using the Hotelling T2 two-sample group difference metric [22], based on covariance matrices. The MANCOVA procedures for the corresponding output 3D color maps of P-values allowed assessment of individual localized morphological variation at different anatomical regions of the condyles. P-values less than 0.05 were considered statistically significant.

RESULTS

Morphological differences between two inbred strains of mice in three different age groups, and between each right and left condyle, were measured and evaluated using three-dimensional (3D) virtual surface models, which allowed for clear visualization of the 3D shape of the articulating surface of the condyles. The use of semi-transparent overlay images helped distinguish individual and group differences.

Tables 3-5 present quantitative assessments of the maximum differences that were obtained when the average morphology at different ages and between different strains of mice (A/J and C3H/HeJ) were compared. Quantification of morphological differences was obtained by 3D signed distances between corresponding surface points. Surface to surface signed distances are displayed as color-coded 3D surface maps where bone remodeling resorptive areas are shown in blue (color-code display standardized for all morphology comparisons at a maximum of -0.105 mm) and bone remodeling apposition

areas are shown in red (color-code display was standardized for all morphology comparisons at a maximum of +0.105 mm). In the different vector maps, the largest absolute distance was set at 0.105 mm, and is shown in red. Morphological differences were measured at eight anatomical regions of interest: anterior, supero-anterior, supero-posterior, posterior, antero-medial, postero-medial, antero-lateral, and postero-lateral. Multivariate analysis of covariance (MANCOVA) 3D color maps of P-values allowed assessment of individual localized morphological variations at different anatomical regions of the condyle. The level of statistical significance was set at 0.05.

Results for Aim 1: Comparison of the articular surface of the mandibular condyle between two different inbred strains of mice (AJ and C3H/HeJ) at 3-5 weeks, 6-8 weeks, and 9-11 weeks of age.

The semi-transparent overlay images showed that on average, the condyles of A/J mice were smaller than those of C3H/HeJ mice at 3-5 weeks of age (Figure 3); morphological comparisons used smaller condyles (A/J strain) as the baseline. The primary difference at this age was observed at the posterior region, with a small increase in size at the anterior and lateral regions. At 6-8 weeks old, C3H/HeJ mice continued to be larger in the posterior region, with a more marked increase in size at the anterior and lateral regions (Figure 4). A comparison between A/J and C3H/HeJ strains of mice at 9-11 weeks showed statistically significant morphological differences (Figure 5). Specifically, condyles of the C3H/HeJ mice were more elongated at the anterior-posterior axis than A/J condyles, with a wider medial-lateral aspect ratio. Condyles of A/J mice presented as more rounded with smaller dimensions.

Results of Aim 2: Comparison of morphological differences in the mandibular condyles of mice at 3-5 weeks, 6-8 weeks, and 9-11 weeks of age for each of two inbred strains of mice.

In the A/J strain, marked condylar growth and morphological changes were observed in mice between 3-5 weeks and 6-8 weeks of age (Figure 6), and both the left and right condyles presented statistically significant elongation of the posterior articulating region. Minimal condylar growth and morphological changes were observed in mice between 6-8 weeks and 9-11 weeks of age (Figure 7). Statistically significant morphological differences were observed in A/J mice between 3-5 weeks and 9-11 weeks old (Figure 8). For C3H/HeJ inbred strains, greater condylar growth and morphological changes were observed in mice between 3-5 weeks and 6-8 weeks of age (Figure 9), and statistically significant differences were noted in mice between 6-8 weeks and 9-11 weeks, especially on the right side. Both the left and right condyles presented statistically significant elongation of the posterior articulating region in mice between 6-8 weeks and 9-11 weeks of age (Figure 10). Morphological comparisons in mice between 3-5 weeks old and 9-11 weeks were highly statistically significant, as shown in Figure 11.

Results for Aim 3: Determine which part of the microanatomy of the condylar articular surface is more stable and less susceptible to morphological variability within each strain and age group.

Condylar articular surfaces that were stable and less susceptible to morphological variability are shown in green in Figures 12-17. Figures 12-14 and 15-17 shows

individual variability within the A/J and CH3/HeJ strains of mice, respectively. In the A/J mice that were 3-5 weeks of age, all 12 (right and left) condyles presented vectors of morphological differences at their anterior articulating surfaces, and nine of the 12 condyles presented differences in the posterior part of the articulating surface; the most stable anatomical regions in the six mice 3-5 weeks of age, were the central portions of the superior, postero-lateral, and postero-medial condylar surfaces (Figure 12). On the left side, one condyle presented with a unique morphology that increased variability in the group. Condyles in A/J mice 6-8 weeks of age presented a consistent pattern of variability at the anterior and antero-superior articulating surfaces; the most stable anatomical regions in the six mice 6-8 weeks of age were the central portions of the superior, postero-lateral, and postero-medial condylar surfaces (Figure 13). The condyles in A/J mice 9-11 weeks of age presented morphological variability localized to the anterior and posterior articulating surfaces. The most stable anatomical regions in the 15 mice at 9-11 weeks were the central portions of the superior, lateral, and medial condylar surfaces (Figure 14).

In C3H/HeJ mice 3-5 weeks of age, the areas that presented with morphological variability were located in the anterior and antero-lateral articulating condylar surfaces, and stable regions were the supero-anterior, supero-posterior, and postero-medial surfaces of all condyles (Figure 15). Condyles in C3H/HeJ mice 6-8 weeks old presented with less stable areas in the anterior region, and stable morphology in the supero-posterior, postero-medial, and postero-lateral surfaces (Figure 16). At 9-11 weeks, less stable regions were located in the anterior and posterior surfaces of the condyles, and the medial and lateral condylar surfaces had stable morphology (Figure 17).

DISCUSSION

Our findings revealed morphological differences in the mandibular condyles of the same genetically inbred strains of mice (AJ and C3H/HeJ) at different ages (3-5 weeks, 6-8 weeks, and 9-11 weeks old). The right and left condyles of the same mouse also presented with some variability in the patterns of the different vector maps. These differences are often referred to as fluctuation asymmetries. Fluctuation asymmetry (FA) originates from small random differences produced during the development of the right and left sides of the body in each individual [23]. The process of analyzing fluctuating asymmetry is a convenient way to control environmental and genetic factors, based on the fact that both sides of the body of an individual have the same genome and are exposed to the same environment. A study by Sheppard (1982) of these asymmetries in a Western population of 286 patients showed condylar asymmetry in 40% of the cases by comparing the right and left condyle in the same mandible. Another study by Capurso and Bonazza (1990) supported these findings. Specifically, the authors evaluated 100 dry Sardinian skulls and found asymmetry in 30% of the mandibular condyles with 13% of the skulls showing glenoid fossa remodeling [24]. Even though we did not obtain asymmetrical percentages of the condyles that we evaluated in mice, we can certainly confirm that there were differences between the right and left condyles of the same mouse in each strain and in all age groups.

Mouse models are most commonly used for studies of human disease and for evaluation of therapeutic strategies. According to Silver (1995), mouse models provide several advantages over other animals; for instance, mice express disease states and characteristics that have a large number of similarities with those found in humans. One

such similarity was demonstrated by Karlo (2010) in his study of mandibles in 210 children, with the use of computer tomography aimed to determine age-related differences in size and shape. His results showed that the growth and development of the condyle in humans is very similar to that observed in mice, and is subject to significant age-related changes in size and shape during childhood, passing from a round shape to a more oval shape [9]. These results were observed in our research as well.

Nevertheless, in genetically heterogeneous populations such as humans, the genetic background and environment has a significant influence on the shape of anatomical structures, making morphometric studies quite difficult. Furthermore, the inability to obtain a large sample of identical twins and to control their environment makes it virtually impossible to carry through with this study. Therefore, it is important, and easier, to use well-characterized animal lines, such as murine inbred strains to study the differences. The genotype and environment of these strains can be strictly controlled, making this strategy important for the study of homogenous populations [1].

A consistent diet has been one of the environmental factors that influence the mandible and condylar shape during its growth and development. Boyd (1990) demonstrated that hard diets expose the temporomandibular joint to great mechanical force during mastication; more so than soft diets [25]. Other authors such as Tuominen (1993) demonstrated in rats that ramus height was greater in rats fed a hard diet than a soft diet[26] , and recently, Enomoto (2009) experimented with mice to determine the influence of mastication on mandibular growth. Enomoto also carried out evaluations using 3D morphometric analyses. He concluded that condylar width (medio-lateral) was

greater in hard diet groups than soft groups, and bone volume was significantly lower in the soft diet group [27].

During our study, quantification of bilateral morphological variability in the articulating surfaces of condyles showed characteristic changes in condylar morphology in mice of different age groups. Mice reach skeletal maturity around 12-16 weeks of age depending on the strain [28]; condylar growth and developmental maturation in the A/J strain mice occurred by 6-8 weeks of age, while in the C3H/HeJ strain mice, marked condylar growth and development continue up to 9-11 weeks, with statistically significant elongation of the posterior articulating region between 6-8 weeks and 9-11 weeks. Characteristic changes over time in both the right and left condyles, from the 3-5 weeks to 9-11 weeks were observed in both AJ and C3H/HeJ mice. The main component of condylar growth appeared to be bone apposition and elongation of the posterior articulating surface. These observed age-related changes are important in determining the approximate age when A/J and C3H/HeJ mice reach condylar maturity, where growth is limited and morphological changes in the condylar area decrease. When we correlate this event to humans, we can infer that *temporomandibular joint (*TMJ) formation in humans begins during embryological development and is completed before age 30; any change after this is considered adaptation to altered functions [24].

The investigation of changes in the morphology of condyles needs to take age range into consideration in order to control anticipated changes due to growth. In this study, quantification of morphological differences in the articulating surfaces of mandibular condyles between the two inbred strains of mice (A/J and C3H/HeJ) at 3-5 weeks, 6-8 weeks, and 9-11 weeks of age revealed interesting findings. Even though both

strains of mice had similar lower jaw sizes (10.8 mm at 15-16 weeks of age), the A/J mice presented with statistically significant smaller condyles than C3H/HeJ mice in all age groups. In addition, it is important to mention that A/J mice had larger skulls (22.8 mm) than C3H/HeJ mice (21.7 mm) at the same age interval of 15-16 weeks [29]. More importantly, these two strains of mice have often been identified as a model system for high bone mass (C3H/HeJ) and low bone mass (A/J) phenotypes [28, 30].

Our study findings revealed that A/J inbred mice presented with condyles that were more round in shape and smaller in size (from the anterior to the posterior pole) than those of C3H/HeJ mice, which presented with a more antero-posteriorly elongated condyles. As seen from a superior view, comparison of the two strains of mice at 3-5 weeks showed no differences in the medio-lateral width of the condyles, but differences became evident and statistically significant in the older mice (6-8 weeks and 9-11 weeks). When we compared these morphological characteristics to the condyle configuration in humans, we observed that the largest human condyle diameter was the medio-lateral region, where we mainly observed major changes in condylar size during the growth and development of the condyle. The antero-posterior region changed and became wider with age, similar to the medio-lateral region of the mouse condyle, which is affected in a similar manner with age as well [9, 31].

Individual variability of condylar morphology was observed in the different vectors between each mouse, and in the average morphology for each strain and age group. In all of the A/J mouse age groups, the most stable condylar surfaces were the central portions of the superior, postero-lateral, and postero-medial surfaces. Individual variability of the anterior articulating condylar surface was also a common finding in

both strains and in all age groups. In C3H/HeJ mice, the 9-11 week old group presented with variability of the superior and posterior articulating surfaces, and only the medio-lateral articulating surface presented with similar morphologies across all condyles. The 3-5 week old group showed morphological variability of the anterior and antero-lateral surfaces, while the stable regions were the supero-anterior, supero-posterior, and postero-medial. The 6-8 week old group demonstrated a less stable anterior region and stable morphology in the supero-posterior, postero-medial, and postero-lateral surfaces in all condyles.

In order to obtain the most accurate microstructure representation, we used micro-CT data, which is considered the "gold standard" to evaluate morphology and bone density in small animal models *in vivo* and *ex vivo*[15, 18]. Schambach (2010) reported that low soft tissue contrast and high radiation doses are the major disadvantages of micro-CT [32]; however, these were not a concern in our study because the data used were *ex vivo*, and we focused on the morphology of the mandibular condyle, and not on soft tissue analysis. Micro-CT allows the analysis of a significantly larger volume compared to two-dimensional (2D) histology, and is a nondestructive imaging technique that allows samples to be used for subsequent assays [16, 33]. While investigations of trabecular morphology may provide additional insight into condylar morphological variability in the two mice models, this is the first study to characterize shape differences between strains of mice with the same genetic background.

CONCLUSIONS

1. Inbred strains of mice are isogenic (homozygous at all loci) and are indistinguishable from all siblings and close relatives, yet they still demonstrated shape differences in the articulating surfaces of their mandibular condyles.
2. Condyles in C3H/HeJ mice were larger than those in A/J mice in the antero-posterior and medio-lateral dimensions of all age groups examined. The greatest differences were observed at near skeletal maturity (9-11 weeks of age).
3. The condyles of A/J mice reached a morphologic plateau around 6-8 weeks of age, while the condyles of C3H/HeJ mice continued to change beyond 6-8 weeks of age.
4. The anterior and the posterior regions of the condyles are the regions that had the greatest variability among A/J and C3H/HeJ mice.

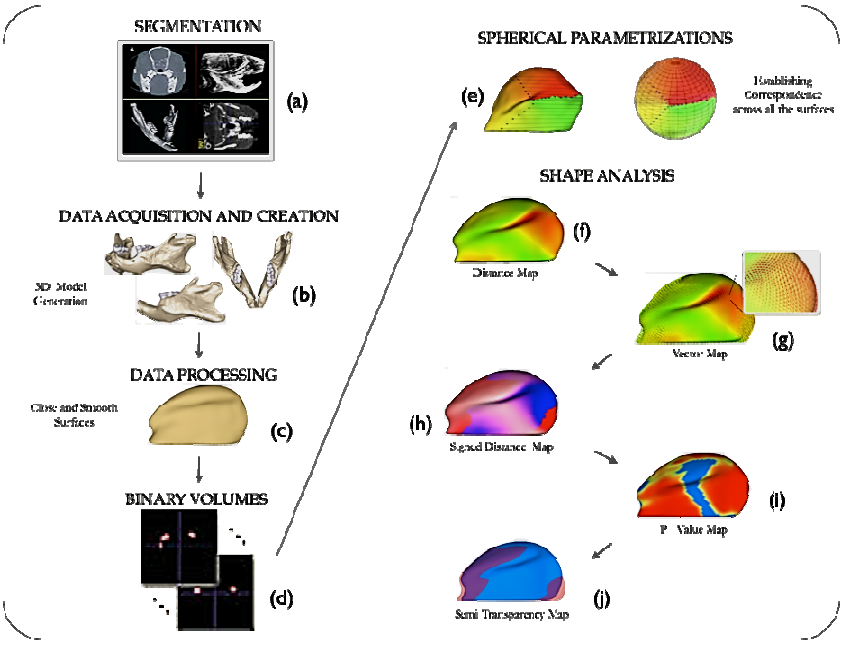

Figure 1: Methodology used for Shape Analysis of the condyles: After the image acquisition with the Micro-CT (a) we can generate the 3D model (b) and continue with the data processing by closure of open "osteotomies" sites and smoothing of the condyle structure(c). This surface information is scanned and converted back to binary volumes (d), and spherical parametrization is established across all condyles in this study sample before using the SPHARM-PDM (e). The Shape analysis software visualizes and quantifies the morphological variability of the condyles utilizing 3D corresponding distance maps (f), vectors maps (g), statistical significance, signed distance maps (h) P-value, maps (i) and Semi-transparency maps (j).

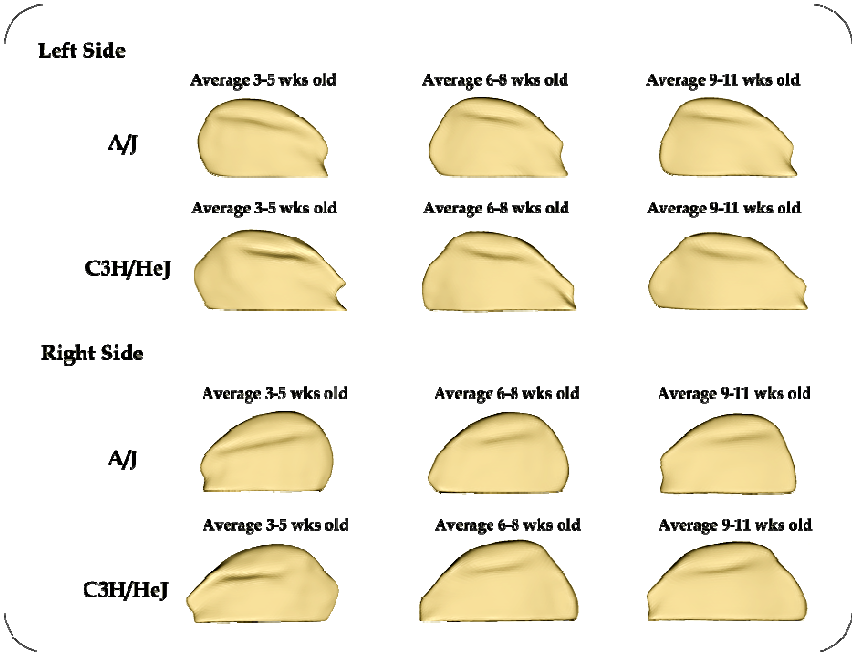

Figure 2: Composites average surface models for each age group, strain and side. Medial view of the condyle's average mesh obtained for each age group 3-5 weeks old, 6-8 weeks old and 9-11 weeks old of each strain A/J and C3H/HeJ and each side (right and left condyles).

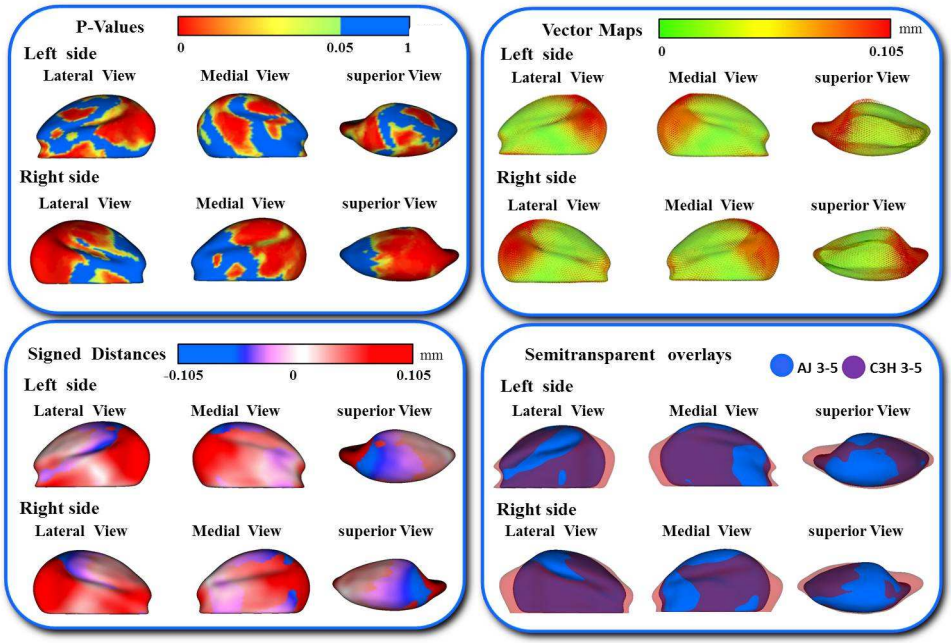

Figure 3: Shape analysis of morphological differences between A/J and C3H/HeJ at 3-5 weeks old mice mandibular condyles. Note that C3H/HeJ condyles had larger dimensions than A/J condyles. The condylar morphology was statistically significantly different on the posterior, supero-posterior, postero-lateral and antero-lateral condylar surfaces; the vector maps showed that the greatest differences were located in posterior and supero-posterior condylar surfaces.

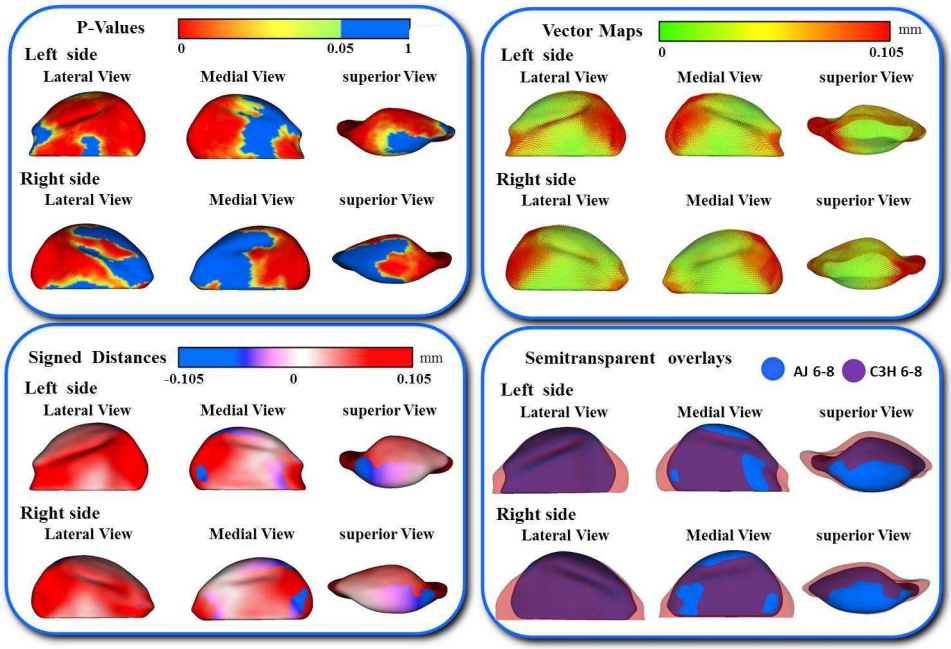

Figure 4: Shape analysis of morphological differences between A/J and C3H/HeJ at 6-8 weeks old mice mandibular condyles. Note that C3H/HeJ condyles had larger dimensions than A/J condyles, and vector maps and semi-transparent overlays reveal similar patterns of differences as shown in the 3-5 week old mice comparisons in Figure 3.

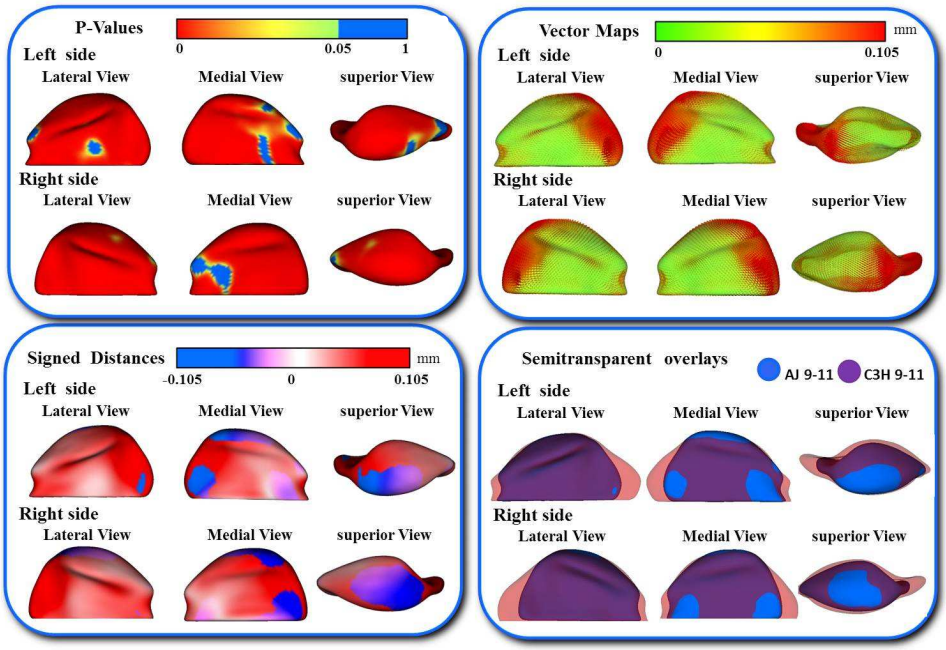

Figure 5: Shape analysis of morphological differences between A/J and C3H/HeJ at 9-11 weeks old mice mandibular condyles. Note that because the C3H/HeJ mice condylar growth continued up to 9-11 weeks of age, at this age the differences between the 2 strains are even more marked, and highly statistically significant.

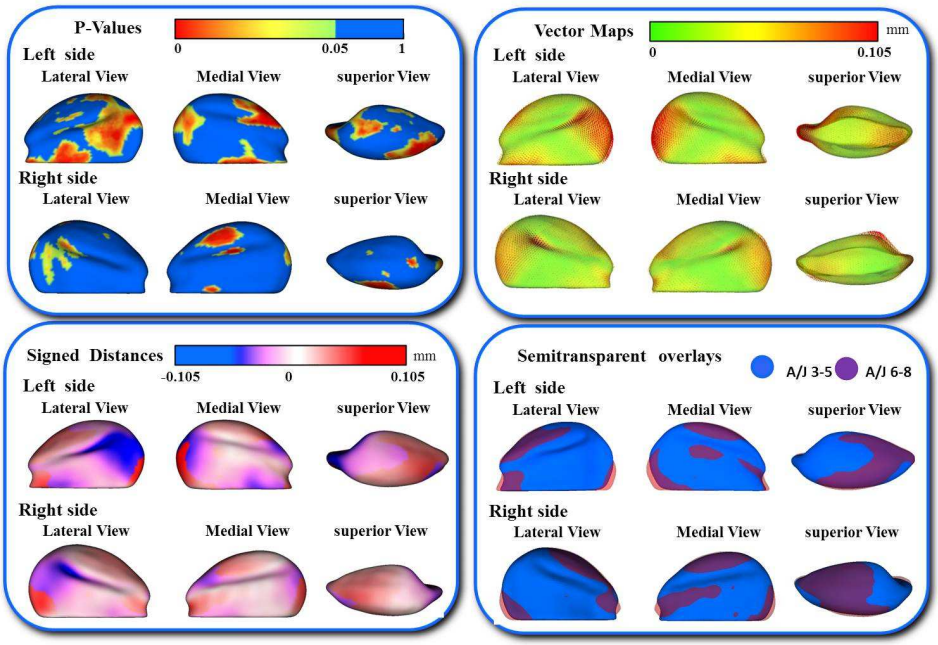

Figure 6: Shape analysis of morphological differences between A/J strain mice condyles at 3-5 weeks old and 6-8 weeks old. Right and left condyles presented with the same pattern of vector differences in the posterior, posterior-superior, postero-lateral and supero-anterior surfaces, but with larger vector differences and statistical significance in the left condyles than the right. Signed distances allowed quantification of areas of morphological and dimensional differences indicative of growth (red) or bone remodeling (resorption in blue). Between 3-5 and 6-8 weeks characteristic surface flattening of the postero-superior surface of the condyles was observed, while elongation indicative of bone growth and apposition between 3-5 and 6-8 weeks was noted in the posterior surfaces.

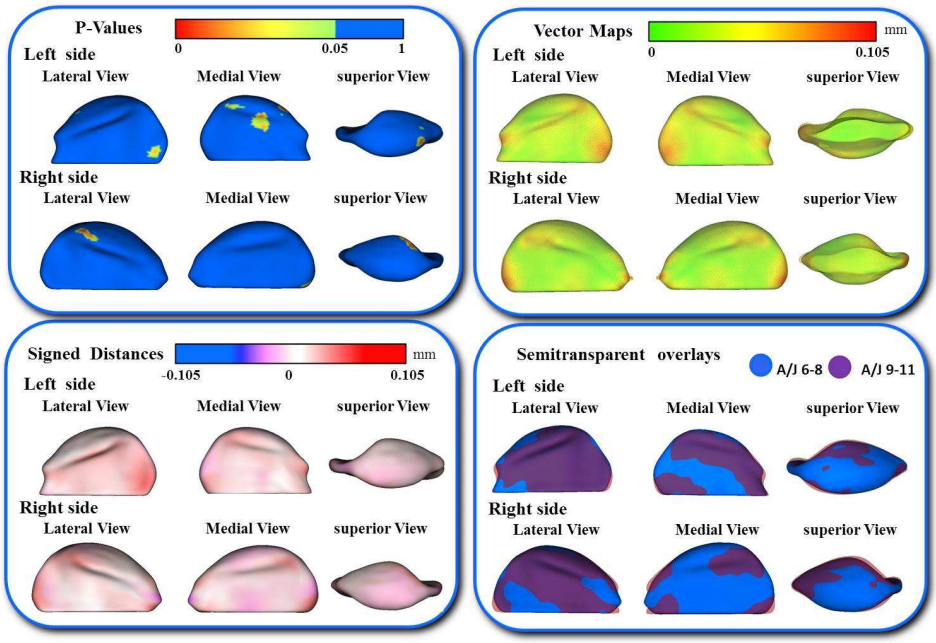

Figure 7: Shape analysis of morphological differences between A/J 6-8 week and 9-11 weeks old mice mandibular condyles. The shape differences during this period were minimal. The P-value maps showed only very small areas of statistically significant changes. The vector maps showed small differences on the posterior and anterior condylar articulating regions.

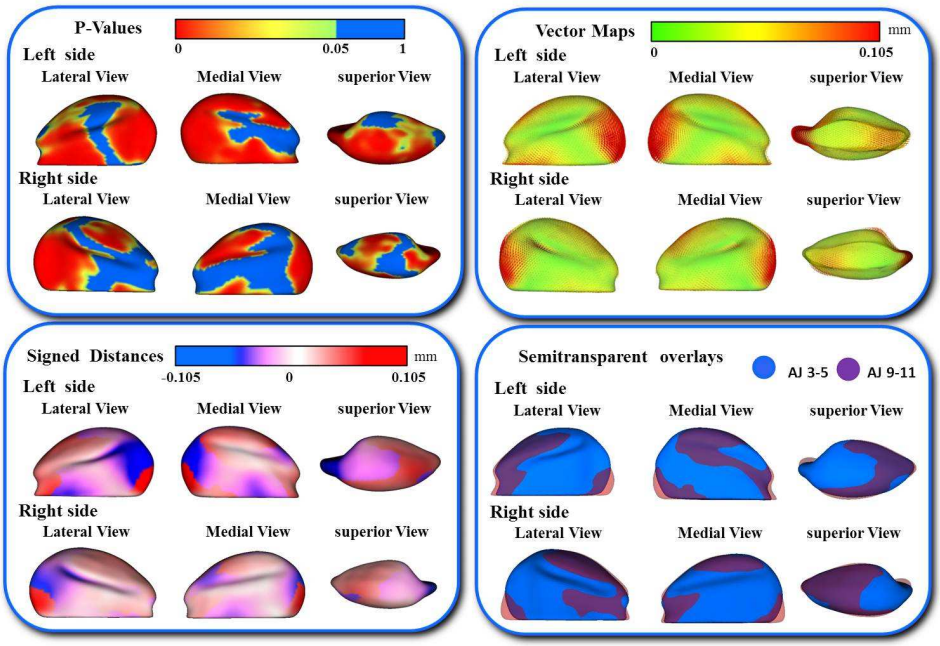

Figure 8: Shape analysis of morphological differences between A/J 3-5 week and 9-11 weeks old mice mandibular condyles. Both left and right condyles presented statistically significant differences on the condylar posterior, supero-posterior, supero-anterior, antero-lateral, antero-medial and postero-medial surfaces. Vector differences were also noticeable at the same anatomic regions. Signed distances and semi-transparencies between 3-5 and 9-11 weeks were similar to the 3-5 and 6-8 week old comparisons in figure 6.

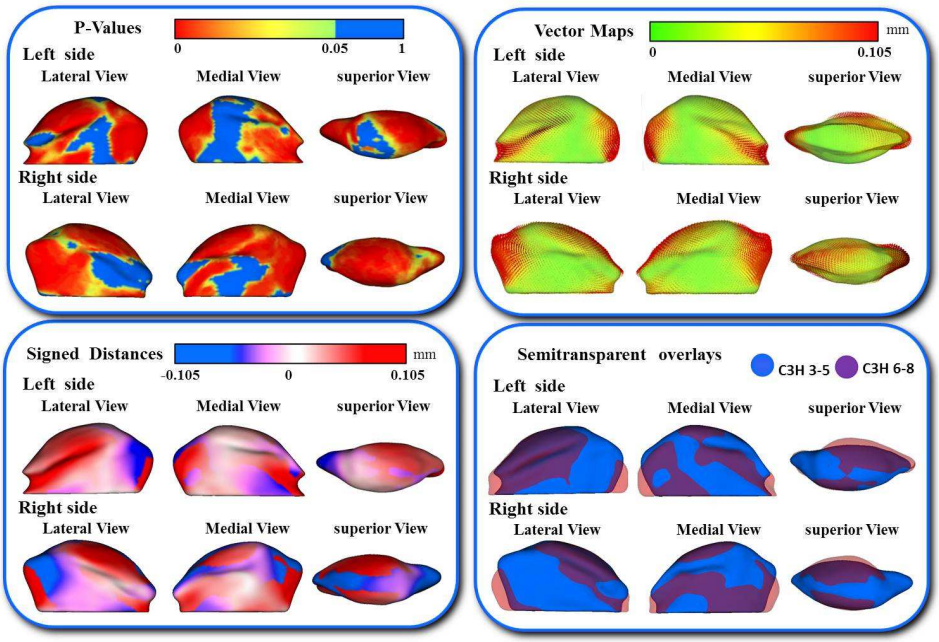

Figure 9: Shape analysis of morphological differences between C3H/HeJ 3-5 weeks old and 6-8 weeks old mice mandibular condyles. The P-value maps showed statistically significant differences in the supero-anterior, supero-posterior, posterior, antero-medial, antero-lateral and postero-lateral condylar surfaces. The vector differences were observed on the same articular surfaces. The signed distance maps showed increased dimensions indicative of bone apposition between 3-5 weeks old and 6-8 weeks on the posterior and anterior condylar surfaces. Areas indicating bone resorption were localized to the supero-posterior condylar surfaces.

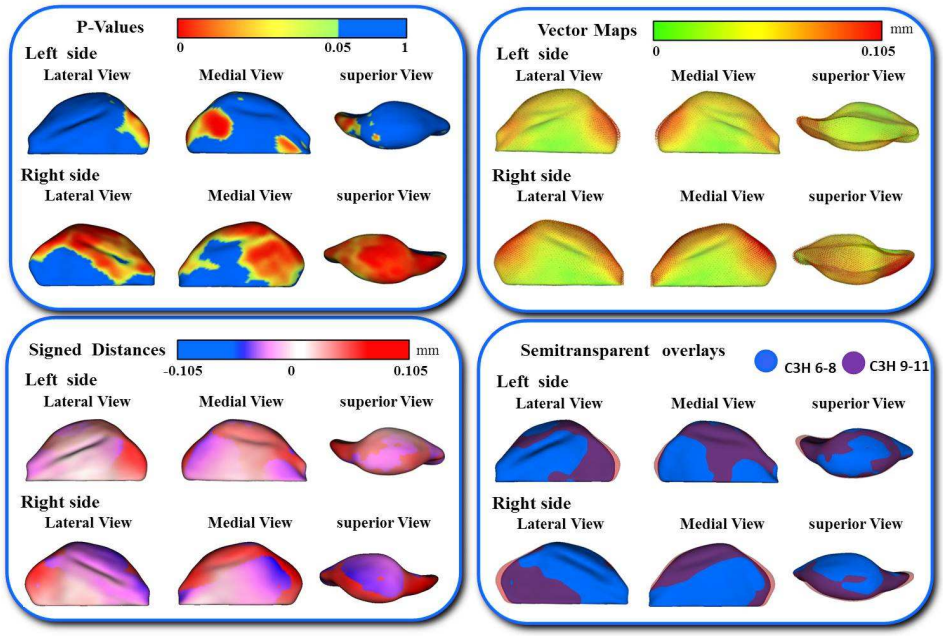

Figure 10: Shape analysis of morphological differences between C3H/HeJ 6-8 weeks old and 9-11 weeks mice mandibular condyles. The P-value maps showed areas of statistically significant morphology in both left and right condyles. Signed distances quantified dimensional differences indicative of bone apposition on the posterior, supero-posterior, postero-medial and antero-medial condylar surfaces; smaller bone remodeling/resorptive differences were measured in the antero-lateral condylar surfaces.

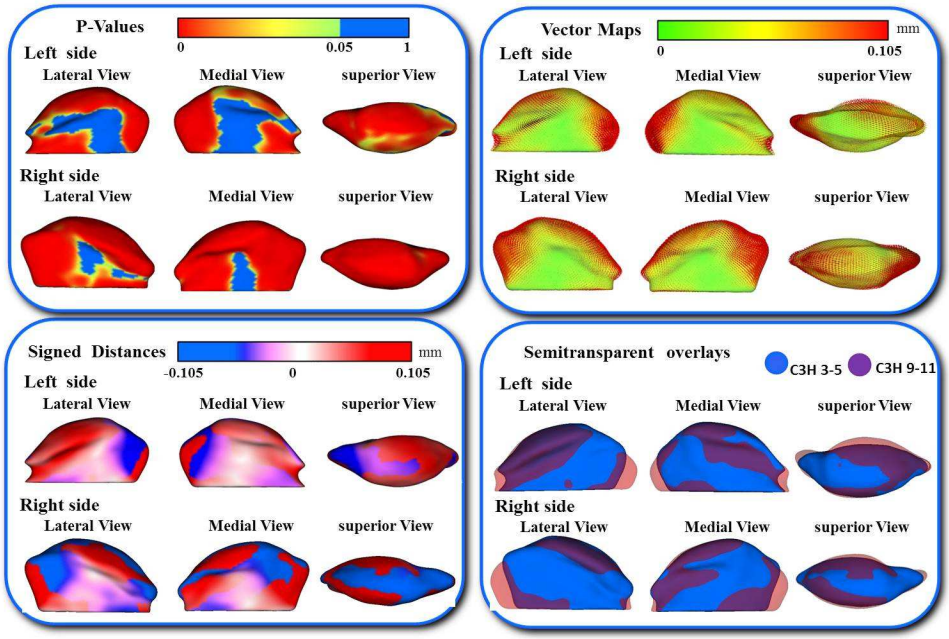

Figure 11: Shape analysis of morphological differences between C3H/HeJ 3-5 weeks old and 9-11 weeks mice mandibular condyles. The morphological differences were highly statistically significant as shown by the P-value maps with more marked changes on the posterior and supero-posterior regions. Signed distances revealed areas of larger dimensions in the 9-11 condyles indicative of bone apposition on the posterior, anterior, supero-anterior, antero-lateral, postero-lateral, and posterior-medial condylar surfaces. Areas indicative of bone resorption were observed on the supero-posterior, postero-medial regions and antero-medial condylar surfaces.

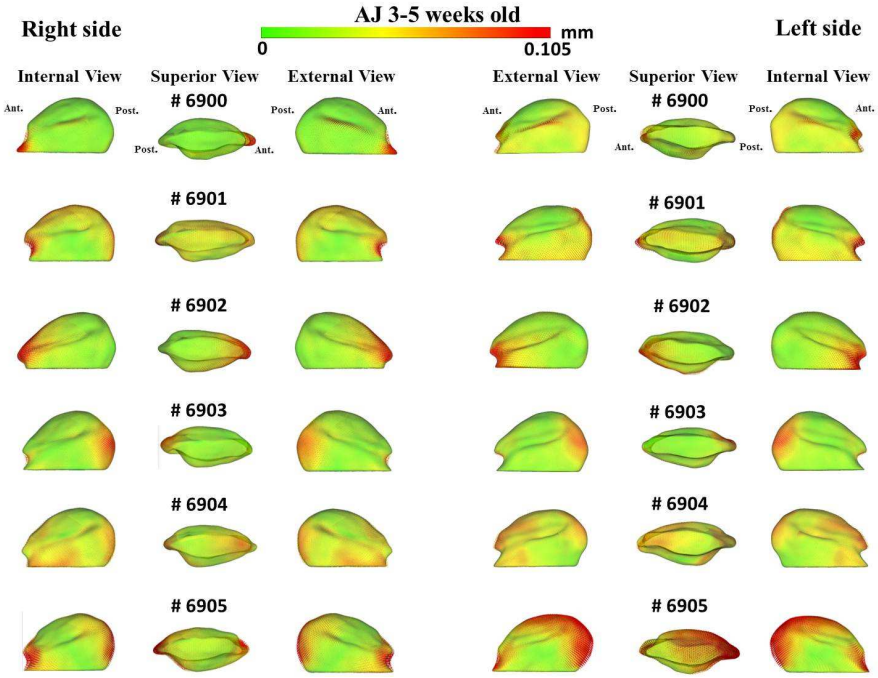

Figure 3: Shape analysis of individual morphological variability of A/J 3-5 weeks old mice mandibular condyles compared to the composite average model. Note that the anterior and posterior surfaces of the condyles showed variability of morphology, as indicated by the difference vectors, while the most stable anatomic regions across the 6 mice at 3-5 weeks were the central portion of the superior, the postero-lateral and the postero-medial condylar surfaces. Also note that the left condyle of mouse #6095 presented a unique morphology with greater variability than all other condyles.

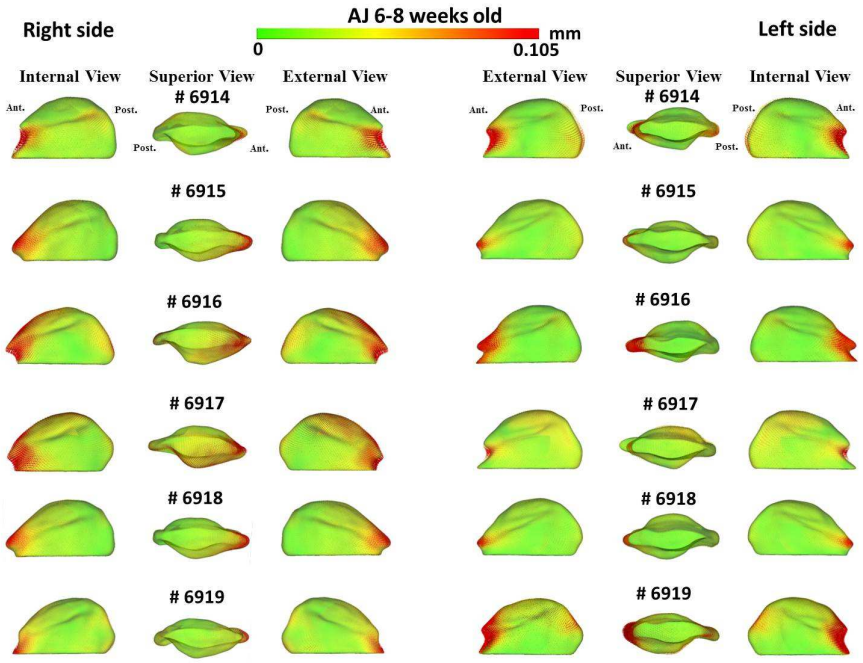

Figure 2: Shape analysis of individual morphological variability of A/J 6-8 weeks old mice mandibular condyles compared to the composite average model. Note that the anterior and antero-superior surfaces of the condyles showed variability of morphology, as indicated by the difference vectors, while the most stable anatomic regions across the 6 mice at 6-8 weeks were the central portion of the superior, the postero-lateral and the postero-medial condylar surfaces, similar to the findings at 3-5 weeks in Figure 12.

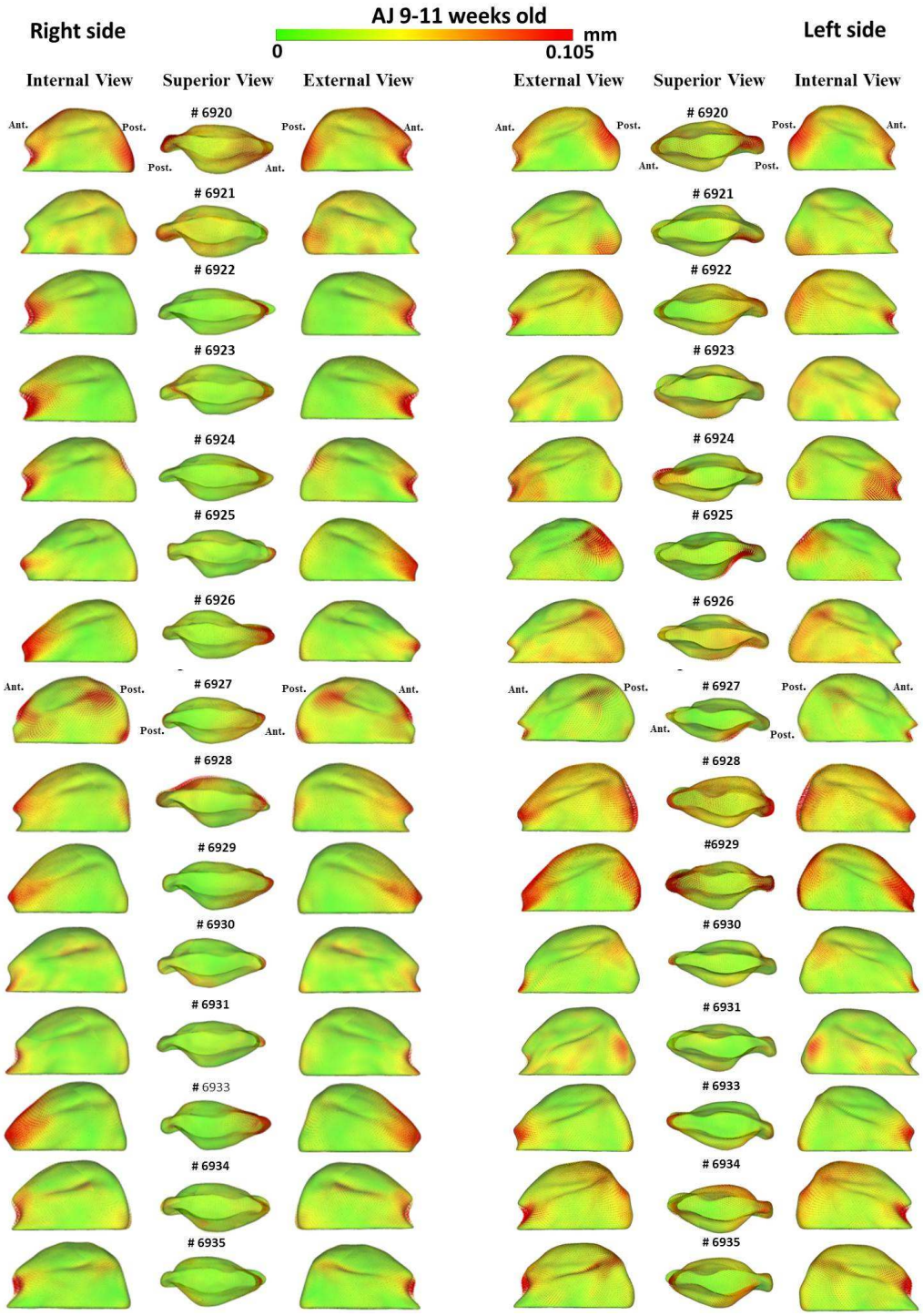

Figure 4: Shape analysis of individual morphological variability of A/J 9-11 weeks old mice mandibular condyles compared to the composite average model. Note that the regions of variability are located in anterior, postero-superior and posterior surfaces of the condyles, while the most stable anatomic regions across the 15 mice at 9-11 weeks were the central portion of the superior, lateral and the medial condylar surfaces.

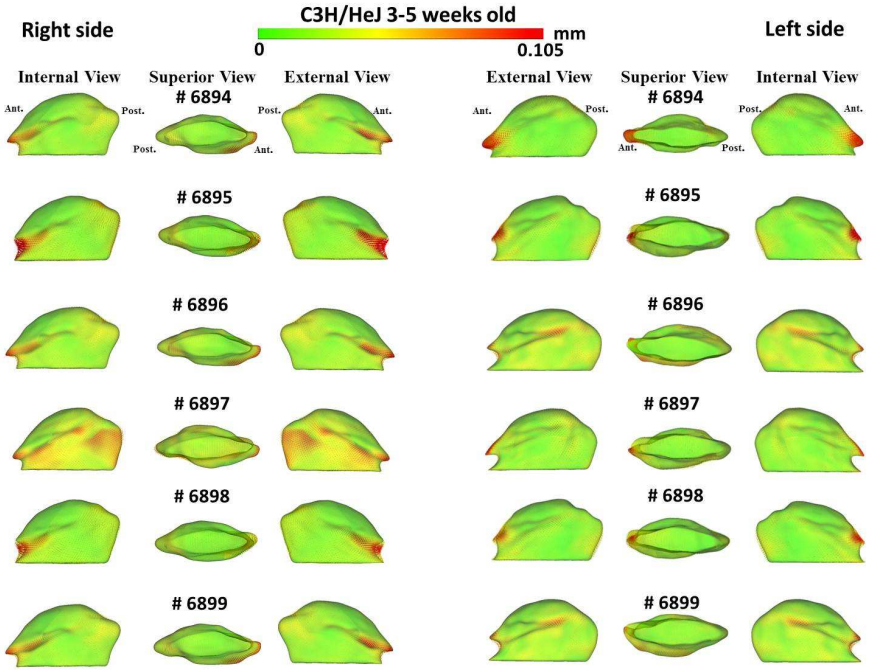

Figure 5: Shape analysis of individual morphological variability of C3H/HeJ 3-5 weeks old mice mandibular condyles compared to the composite average model. Note that the anterior and antero-lateral surfaces of the condyles showed variability of morphology, as indicated by the difference vectors, while the most stable anatomic regions were the supero-anterior, supero-posterior, postero-lateral and the postero-medial condylar surfaces.

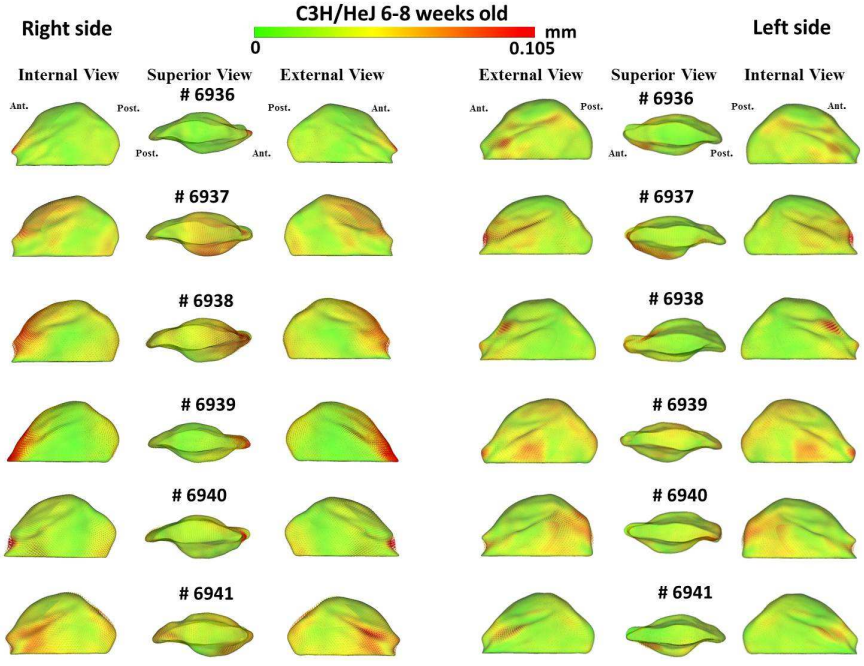

Figure 6: Shape analysis of individual morphological variability of C3H/HeJ 6-8 weeks old mice mandibular condyles compared to the composite average model. Note that the anterior surfaces of the condyles showed variability of morphology, as indicated by the difference vectors, while the most stable anatomic regions were the supero-posterior, postero-lateral and postero-medial condylar surfaces.

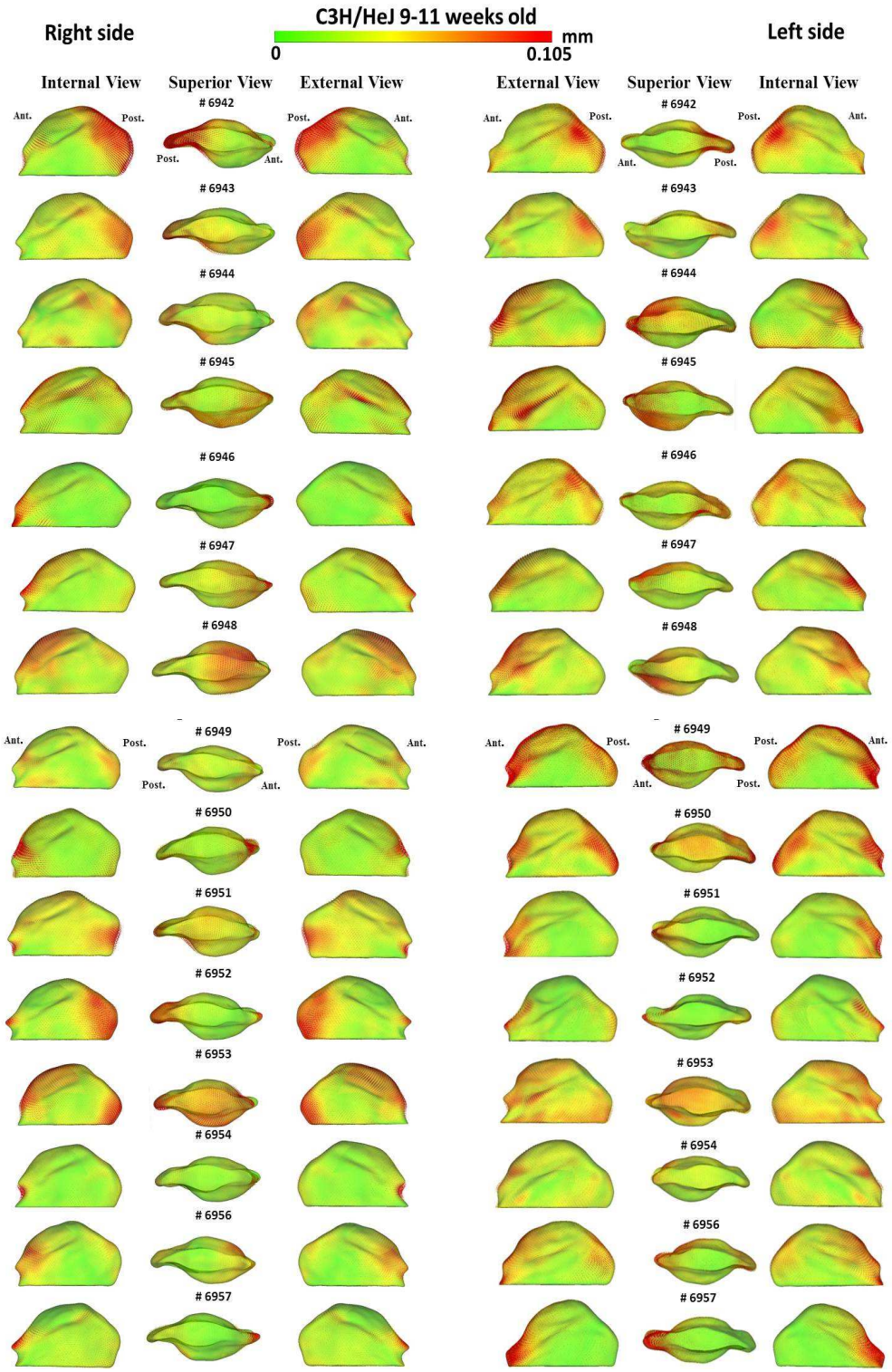

Figure 7: Shape analysis of individual morphological variability of C3H/HeJ 9-11 weeks old mice mandibular condyles compared to the composite average model. Note that the anterior and posterior surfaces showed more variability, while the medial and lateral condylar surfaces had stable morphology.

Table 3: Maximum difference values of the right and left mean average composite model comparison between A/J and C3H/HeJ strains at three different age groups, 3-5 weeks old, 6-8 weeks old and 9-11 weeks

	Anterior	Supero Anterior	Supero Posterior	Posterior	Antero Medial	Postero Medial	Antero Lateral	Postero Lateral
Right Condyle								
A/J - C3H/HEJ 3-5 wks	-0.1076	-0.0473	-0.1933 *	-0.1544 *	-0.0521	-0.0797 *	-0.0695	0.074 *
A/J - C3H/HEJ 6-8 wks	-0.1136	-0.0405	0.1641 *	-0.2464 *	-0.0339	-0.0731	-0.1014 *	-0.0736 *
A/J - C3H/HEJ 9-11 wks	0.1205 *	0.0665*	0.1887 *	0.2973 *	0.0826 *	0.1039 *	0.0666 *	0.0556 *
Left Condyle								
A/J - C3H/HEJ 3-5 wks	-0.0843	-0.0331	-0.1644 *	-0.1317 *	0.0512 *	-0.0699	0.0162 *	0.0982
A/J - C3H/HEJ 6-8 wks	-0.1701	-0.0474	-0.1803 *	-0.2025 *	0.0137	0.0609	-0.1035 *	-0.0925 *
A/J - C3H/HEJ 9-11 wks	-0.1132 *	-0.0516 *	-0.2483 *	-0.2394 *	-0.0536 *	-0.0922 *	-0.0678 *	-0.0831 *

Multivariate analysis of covariance (MANCOVA) were used to test whether mean group morphology models were statistically significantly different when we compared A/J and C3H/HEJ mouse strains at 3 different age group. The P-value maps for testing a group's differences were calculated using the Hotelling T2 metric, based on covariance matrices. (*) Statistical significance value was set at $P \leq 0.05$

Table 4: Maximum difference values of the right and left mean average composite model comparison among A/J strains of mice at three different age groups, 3-5 weeks old, 6-8 weeks old and 9-11 weeks old

	Anterior	Supero Anterior	Supero Posterior	Posterior	Antero Medial	Postero Medial	Antero Lateral	Postero Lateral
Right Condyle								
A/J 3-5 wks - A/J 9-11 wks	0.0526	-0.059 *	0.0706 *	-0.1339 *	0.0616 *	-0.0319	0.0321 *	-0.0156
A/J 3-5 wks - A/J 6-8 wks	-0.0799	-0.0522	0.0355 *	-0.0784	0.0468 *	0.0191	0.0271	0.0754 *
A/J 6-8 wks - A/J 9-11 wks	0.0634	0.0127	0.0422	0.0553	0.0231	0.0315	0.0102	0.0346 *
Left Condyle								
A/J 3-5 wks - A/J 9-11 wks	0.0617	0.0851 *	0.1369 *	0.141 *	0.0851 *	0.0387 *	0.0322 *	0.1077
A/J 3-5 wks - A/J 6-8 wks	0.0155	0.0725 *	-0.1181 *	0.1031	-0.0782 *	0.0134	-0.0334	-0.1382 *
A/J 6-8 wks - A/J 9-11 wks	0.0464	-0.0168	-0.2701	0.0469	0.0173 *	0.0352	0.0289	0.0403

Multivariate analyses of covariance (MANCOVA) were used to test whether mean group morphology models were statistically significantly different when we compared A/J strains at 3 different age groups. The P-value maps for testing a group's differences were calculated using the Hotelling T2 metric, based on covariance matrices. (*) Statistical significance value was set at $P \leq 0.05$.

Table 5: Maximum difference values of the right and left mean average composite model comparison among C3H/HeJ strains of mice at three different age groups, 3-5 weeks old, 6-8 weeks old and 9-11 weeks

	Anterior	Supero Anterior	Supero Posterior	Posterior	Antero Medial	Postero Medial	Antero Lateral	Postero Lateral
Right Condyle								
C3H/HeJ 3-5 wks - C3H/HeJ 911 wks	0.1415 *	0.1764 *	0.2203 *	-0.2731 *	0.1288 *	0.105 *	0.0687 *	0.0532 *
C3H/HeJ 3-5 wks - C3H/HeJ 6-8 wks	-0.1021	0.1181 *	0.1993	-0.2013	0.0864 *	0.0617 *	-0.061	-0.0752 *
C3H/HeJ 6-8 wks - C3H/HeJ 9-11 wks	0.0873 *	-0.0894 *	-0.0957 *	-0.0693 *	-0.0691	-0.0783 *	0.0557	0.0589 *
Left Condyle								
C3H/HeJ 3-5 wks - C3H/HeJ 911 wks	0.1394 *	0.0963 *	-0.1864 *	0.2294 *	0.072 *	0.0584	0.1089 *	0.0973 *
C3H/HeJ 3-5 wks - C3H/HeJ 6-8 wks	0.1713 *	0.0756 *	-0.1241 *	0.1902 *	0.0469 *	0.0144	0.1021 *	0.1113 *
C3H/HeJ 6-8 wks - C3H/HeJ 9-11 wks	-0.0525	0.0624	0.0812 *	0.0867 *	0.0574	0.0509	-0.2428	0.0284

Multivariate analysis of covariance (MANCOVA) were used to test whether mean group morphology models were statistically significantly different when we compared among C3H/HeJ mouse strains at 3 different age group. The P-value maps for testing a group's differences were calculated using the Hotelling T2 metric, based on covariance matrices. (*) Statistical significance value was set at $P \leq 0.05$

REFERENCES

1. Gama Sosa, M.A., R. De Gasperi, and G.A. Elder, *Animal transgenesis: an overview.* Brain Struct Funct, 2010. **214**(2-3): p. 91-109.

2. Klingenberg, C.P., L.J. Leamy, and J.M. Cheverud, *Integration and modularity of quantitative trait locus effects on geometric shape in the mouse mandible.* Genetics, 2004. **166**(4): p. 1909-21.

3. Atchley, W.R. and B.K. Hall, *A model for development and evolution of complex morphological structures.* Biological reviews of the Cambridge Philosophical Society, 1991. **66**(2): p. 101-57.

4. Festing, M., *Mouse strain identification.* Nature, 1972. **238**(5363): p. 351-2.

5. Rodrigues, J.H., D.A. Biasotto-Gonzalez, S.K. Bussadori, R.A. Mesquita-Ferrari, K.P. Fernandes, C.A. Tenis, and M.D. Martins, *Signs and symptoms of temporomandibular disorders and their impact on psychosocial status in non-patient university student's population.* Physiotherapy research international : the journal for researchers and clinicians in physical therapy, 2012. **17**(1): p. 21-8.

6. Mohlin, B., B. Ingervall, and B. Thilander, *Relation between malocclusion and mandibular dysfunction in Swedish men.* The European Journal of Orthodontics, 1980. **2**(4): p. 229-238.

7. Alexiou, K., H. Stamatakis, and K. Tsiklakis, *Evaluation of the severity of temporomandibular joint osteoarthritic changes related to age using cone beam computed tomography.* Dentomaxillofac Radiol, 2009. **38**(3): p. 141-7.

8. Yura, S., K. Ooi, S. Kadowaki, Y. Totsuka, and N. Inoue, *Magnetic resonance imaging of the temporomandibular joint in patients with skeletal open bite and subjects with no dentofacial abnormalities.* The British journal of oral & maxillofacial surgery, 2010. **48**(6): p. 459-61.

9. Karlo, C.A., P. Stolzmann, S. Habernig, L. Müller, T. Saurenmann, and C.J. Kellenberger, *Size, shape and age-related changes of the mandibular condyle during childhood.* European radiology, 2010. **20**(10): p. 2512-2517.

10. Gatchel, R.J., A.W. Stowell, L. Wildenstein, R. Riggs, and E. Ellis, 3rd, *Efficacy of an early intervention for patients with acute temporomandibular disorder-related pain: a one-year outcome study.* J Am Dent Assoc, 2006. **137**(3): p. 339-47.

11. Barbosa, T.d.S., L.S. Miyakoda, R.d.L. Pocztaruk, C.P. Rocha, and M.B.D. Gavião, *Temporomandibular disorders and bruxism in childhood and*

adolescence: Review of the literature. International Journal of Pediatric Otorhinolaryngology, 2008. **72**(3): p. 299-314.

12. Kanehira, H., A. Agariguchi, H. Kato, S. Yoshimine, and H. Inoue, *Association between stress and temporomandibular disorder.* Nihon Hotetsu Shika Gakkai Zasshi, 2008. **52**(3): p. 375-80.

13. Drangsholt, M.T., *Psychological characteristics such as depression, independent from a known genetic risk factor, increase the risk of developing temporomandibular disorder pain.* The journal of evidence-based dental practice, 2008. **8**(4): p. 240-1.

14. Helenius, L.M., D. Hallikainen, I. Helenius, J.H. Meurman, M. Kononen, M. Leirisalo-Repo, and C. Lindqvist, *Clinical and radiographic findings of the temporomandibular joint in patients with various rheumatic diseases. A case-control study.* Oral surgery, oral medicine, oral pathology, oral radiology, and endodontics, 2005. **99**(4): p. 455-63.

15. Ritman, E.L., *Micro-computed tomography-current status and developments.* Annual review of biomedical engineering, 2004. **6**: p. 185-208.

16. Bouxsein, M.L., S.K. Boyd, B.A. Christiansen, R.E. Guldberg, K.J. Jepsen, and R. Müller, *Guidelines for assessment of bone microstructure in rodents using micro-computed tomography.* Journal of Bone and Mineral Research, 2010. **25**(7): p. 1468-1486.

17. Muller, R., H. Van Campenhout, B. Van Damme, G. Van Der Perre, J. Dequeker, T. Hildebrand, and P. Ruegsegger, *Morphometric analysis of human bone biopsies: a quantitative structural comparison of histological sections and micro-computed tomography.* Bone, 1998. **23**(1): p. 59-66.

18. Feldkamp, L.A., S.A. Goldstein, A.M. Parfitt, G. Jesion, and M. Kleerekoper, *The direct examination of three-dimensional bone architecture in vitro by computed tomography.* J Bone Miner Res, 1989. **4**(1): p. 3-11.

19. Yushkevich, P.A., J. Piven, H.C. Hazlett, R.G. Smith, S. Ho, J.C. Gee, and G. Gerig, *User-guided 3D active contour segmentation of anatomical structures: significantly improved efficiency and reliability.* Neuroimage, 2006. **31**(3): p. 1116-28.

20. Styner, M., I. Oguz, S. Xu, C. Brechbuhler, D. Pantazis, J.J. Levitt, M.E. Shenton, and G. Gerig, *Framework for the Statistical Shape Analysis of Brain Structures using SPHARM-PDM.* The insight journal, 2006(1071): p. 242-250.

21. Paniagua, B., L. Cevidanes, H. Zhu, and M. Styner, *Outcome quantification using SPHARM-PDM toolbox in orthognathic surgery.* Int J Comput Assist Radiol Surg, 2010.

22. Styner, M., I. Oguz, S. Xu, D. Pantazis, and G. Gerig. *Statistical group differences in anatomical shape analysis using Hotelling T2 metric*. in *Medical Imaging*. 2007. International Society for Optics and Photonics.

23. Greene, D.L., *Fluctuating dental asymmetry and measurement error.* American journal of physical anthropology, 1984. **65**(3): p. 283-9.

24. Scafoglieri, A., P. Van Roy, and J.P. Clarijs, *[Left-right asymmetries and other common anatomical variants of temporomandibular articular surfaces]*. Nederlands tijdschrift voor tandheelkunde, 2008. **115**(1): p. 14-21.

25. Boyd, R.L., C.H. Gibbs, P.E. Mahan, A.F. Richmond, and J.L. Laskin, *Temporomandibular joint forces measured at the condyle of Macaca arctoides.* American journal of orthodontics and dentofacial orthopedics : official publication of the American Association of Orthodontists, its constituent societies, and the American Board of Orthodontics, 1990. **97**(6): p. 472-9.

26. Tuominen, M., T. Kantomaa, and P. Pirttiniemi, *Effect of food consistency on the shape of the articular eminence and the mandible. An experimental study on the rabbit.* Acta odontologica Scandinavica, 1993. **51**(2): p. 65-72.

27. Enomoto, A., J. Watahiki, T. Yamaguchi, T. Irie, T. Tachikawa, and K. Maki, *Effects of mastication on mandibular growth evaluated by microcomputed tomography.* The European Journal of Orthodontics, 2009. **32**(1): p. 66-70.

28. Voide, R., G.H. van Lenthe, and R. Müller, *Differential Effects of Bone Structural and Material Properties on Bone Competence in C57BL/6 and C3H/He Inbred Strains of Mice.* Calcified Tissue International, 2008. **83**(1): p. 61-69.

29. Donahue, L., *Bone mineral density, body composition, and craniofacial characterization in 30 inbred strains of mice. ,* in *Mouse Phenome Database web site, The Jackson Laboratory, Bar Harbor, Maine USA. http://phenome.jax.org*, May, 2011.

30. Ng, A.H., S.X. Wang, C.H. Turner, W.G. Beamer, and M.D. Grynpas, *Bone quality and bone strength in BXH recombinant inbred mice.* Calcified Tissue International, 2007. **81**(3): p. 215-23.

31. Tadej, G., C. Engstrom, H. Borrman, and E.L. Christiansen, *Mandibular condyle morphology in relation to malocclusions in children.* The Angle Orthodontist, 1989. **59**(3): p. 187-194.

32. Schambach, S.J., S. Bag, L. Schilling, C. Groden, and M.A. Brockmann, *Application of micro-CT in small animal imaging.* Methods, 2010. **50**(1): p. 2-13.

33. Waarsing, J.H., J.S. Day, and H. Weinans, *An Improved Segmentation Method for In Vivo μCT Imaging.* Journal of Bone and Mineral Research, 2004. **19**(10): p. 1640-1650.